Article

Transdifferentiation of plasmatocytes to crystal cells in the lymph gland of *Drosophila melanogaster*

Julien Marcetteau[1,5], Patrícia Duarte[1,5], Alexandre B Leitão [ID] [2✉] & Élio Sucena [ID] [1,3,4✉]

Abstract

Under homeostatic conditions, haematopoiesis in *Drosophila* larvae occurs in the lymph gland and sessile haemocyte clusters to produce two functionally and morphologically different cells: plasmatocytes and crystal cells. It is well-established that in the lymph gland both cell types stem from a binary decision of the medullary prohaemocyte precursors. However, in sessile clusters and dorsal vessel, crystal cells have been shown to originate from the transdifferentiation of plasmatocytes in a Notch/Serrate-dependent manner. We show that transdifferentiation occurs also in the lymph gland. In vivo phagocytosis assays confirm that cortical plasmatocytes are functionally differentiated phagocytic cells. We uncover a double-positive population in the cortical zone that lineage-tracing and long-term live imaging experiments show will differentiate into crystal cells. The reduction of Notch levels within the lymph gland plasmatocyte population reduces crystal cell number. This extension of a transdifferentiation mechanism reinforces the growing role of haematopoietic plasticity in maintaining homeostasis in *Drosophila* and vertebrate systems. Future work should test the regulation and relative contribution of these two processes under different immunological and/or metabolic conditions.

Introduction

Under homeostatic conditions, haematopoiesis in *Drosophila melanogaster* produces two functionally distinct, mature haemocyte classes: plasmatocytes and crystal cells (Rizki, 1957). Plasmatocytes are macrophage-like cells and makeup approximately 90–95% of the haemocyte population whilst crystal cells are larger, post-mitotic cells which produce prophenoloxidase and constitute the remaining 5–10% (Rizki, 1957, 1959; Lanot et al, 2001; Evans et al, 2003; Banerjee et al, 2019). These two cell populations have been typically distinguished based on their morphology (Rizki, 1957;

Shrestha and Gateff, 1982; Lanot et al, 2001) and through the expression of a range of specific markers and corresponding drivers (Lebestky et al, 2000; Kurucz et al, 2007; Evans et al, 2014). Several recent studies revealed that this classic classification may be overly simplistic, as single-cell transcriptomics and functional studies revealed that haemocytes cluster into a larger number of categories than originally thought (Cattenoz et al, 2020; Cho et al, 2020; Fu, 2020; Leitão et al, 2020; Tattikota et al, 2020; Girard et al, 2021; Coates et al, 2021; preprint: Brooks et al, 2024). Nonetheless, this knowledge does not contradict, but rather confirms, the notion that mature plasmatocytes express diagnostic markers such as the phagocytosis receptors Eater and NimrodC1 (Kocks et al, 2005; Kurucz et al, 2007; Hultmark and Andó 2022). The same applies to crystal cells, which can be identified by their expression of the RUNX transcription factor Lozenge (Lebestky et al, 2000) and activity driven by the crystal cell-specific enhancer, BcF6 (Tokusumi et al, 2009).

The first stage of haematopoiesis takes place in embryonic development, during which a population of cells of the pro-cephalic mesoderm adopts haemocyte fate (Holz et al, 2003). Haemocytes of this population subsequently migrate into the hemocoel (Tepass et al, 1994), into the haematopoietic pockets and into dorsal vessel-associated clusters (Makhijani et al, 2011). These cells persist throughout larval life and into adulthood (Holz et al, 2003; Wood and Jacinto, 2007; Letourneau et al, 2016). Also, during embryogenesis, lymph gland development is initiated from the cardiogenic mesoderm as a series of bilaterally symmetrical lobes, which flank the anterior end of the dorsal vessel (Rugendorff et al, 1994; Grigorian and Hartenstein, 2013). Throughout larval life, a second stage of haematopoiesis will take place in the lymph gland, primarily in the most anterior primary lobes. These comprise a medullary zone containing undifferentiated prohaemocytes surrounded by a cortical zone of maturing and mature haemocytes (Shrestha and Gateff, 1982; Leitão and Sucena, 2015, Jung et al, 2005; Crozatier and Meister, 2007; Blanco-Obregon et al, 2020; Kharrat et al, 2022). In addition, haematopoiesis occurs in the segmentally organized, sub-epidermal sessile haemocyte clusters of the larva (Márkus et al, 2009; Makhijani et al, 2011; Bretscher et al, 2015; Gold and Brückner, 2015; Leitão and Sucena, 2015) and, arguably, in the adult (see (Ghosh et al, 2015) versus (Sanchez Bosch et al, 2019)).

The classic haematopoiesis model establishes that the fate of prohaemocytes is defined through a binary decision between plasmatocyte and crystal cell differentiation programs

[1]Instituto Gulbenkian de Ciência, Rua da Quinta Grande 6, 2780-156 Oeiras, Portugal. [2]Fundação Champalimaud, Lisboa, Portugal. [3]Departamento de Biologia Animal, Faculdade de Ciências, Universidade de Lisboa, Edifício C2, Campo Grande, 1749-016 Lisbon, Portugal. [4]cE3c: Centre for Ecology, Evolution and Environmental Changes, Faculdade de Ciências, Universidade de Lisboa, Campo Grande, 1749-016 Lisbon, Portugal. [5]These authors contributed equally: Julien Marcetteau, Patrícia Duarte. ✉E-mail: alexandre.leitao@research.fchampalimaud.org; jesucena@fc.ul.pt

(Lebestky et al, 2000; Duvic et al, 2002; Krzemien et al, 2010a; Banerjee et al, 2019). This happens as early as during early second instar larvae (L2) when the cortical zone matures and involving intermediate cell types (Kocks et al, 2005; Sinenko et al, 2009; Krzemien et al, 2010a, 2010b; Ferguson and Martinez-Agosto, 2014; Blanco-Obregon et al, 2020; Spratford et al, 2021). Strong evidence has accumulated to sustain that Notch pathway activation, through its ligand Serrate, is necessary for crystal cell differentiation. This process appears to be restricted to the cortical zone of the lymph gland (Duvic et al, 2002; Lebestky et al, 2003; Jung et al, 2005; Blanco-Obregon et al, 2020) and the sessile haemocyte clusters (Leitão and Sucena, 2015). Interestingly, in the sessile clusters, crystal cells arise de novo through the Notch-dependent transdifferentiation of mature plasmatocytes (Leitão and Sucena, 2015), a finding that does not fit with the original "binary decision model" of crystal cell differentiation from a haemocyte precursor. More recently, this alternative mechanism of crystal cell production has been shown to also occur in the dorsal vessel (Cevik et al, 2019), and to possibly depend on oxygen-sensing neurons in sessile clusters that surround the caudal sensory cones (preprint: Corcoran et al, 2020). Importantly, this transdifferentiation process is also established for lamellocyte production, as shown by the Hultmark and Andó laboratories (Honti et al, 2010; Anderl et al, 2016; Csordás et al, 2021) and further reinforced in recent studies (Cho et al, 2020; Tattikota et al, 2020). Indeed, scRNA-seq data has shown that haemocyte populations, once subclustered and ordered along a pseudotemporal scale, exhibit lineages ranging from self-cycling plasmatocytes to terminal fate crystal cells fate or lamellocytes. More importantly, single-cell transcriptomic data related exclusively to the lymph gland suggests the existence of a plasmatocyte subpopulation with the potential to transdifferentiate into crystal cells, within this organ (Cho et al, 2020; Girard et al, 2021).

In light of this accumulated evidence in sessile clusters and dorsal vessel for a Notch-dependent plasmatocyte-to-crystal cell transdifferentiation process, we tested for its extension to the lymph gland, the main *Drosophila* haematopoietic organ.

Results

Cortical plasmatocytes transdifferentiate into crystal cells in a Notch-dependent manner

Notch activation is necessary and sufficient for crystal cell differentiation in the lymph gland (Lebestky et al, 2000, 2003; Duvic et al, 2002; Small et al, 2014) and necessary in the sessile clusters for the transdifferentiation of mature plasmatocytes into crystal cell (Leitão and Sucena, 2015). If transdifferentiation is taking place also in the lymph gland, several predictions ensue. First, Notch activation should be restricted to the cortical zone, which is to say, detectable only in cortical plasmatocytes; second, intermediate-stage cells should be found, i.e., expressing terminal differentiation markers; lastly, interfering with Notch activity in cortical plasmatocytes should reduce crystal cell numbers. In order to test these predictions, we took advantage of the Notch responsive element reporter line (NRE-eGFP).

First, combining NRE-eGFP with HmlΔ-DsRed (a cell marker that starts its expression in maturing haemocytes) and observing 12 dissected lymph glands could not reveal NRE-eGFP expression in the medullary zone, which hosts undifferentiated haemocytes (Fig. EV1A,a′). The restricted expression pattern of Notch activity to the intermediate and cortical zone of Hml+ haemocytes is consistent with crystal cell differentiation not occurring in the medullary zone.

A transdifferentiation model predicts the existence of a transient cell type, which simultaneously, or sequentially, expresses mature plasmatocyte and Notch activity markers. We stained lymph glands from L3 larvae carrying the NRE-eGFP reporter with the P1 antibody, specific against the Nimrod membrane protein expressed in differentiated phagocytically active plasmatocytes (Vilmos, 2004; Kurucz et al, 2007; Terriente-Felix et al, 2013) confirming the existence of a qualitatively distinct population of plasmatocytes activated for Notch in the cortical zone of the lymph glands (Fig. 1A,1a'). The predicted transient nature of this cell type could be verified further by quantifying each of the three cell populations expected under a transdifferentiation model: plasmatocytes (P1$^+$ NRE$^-$), committed crystal cells (P1$^-$ NRE$^+$) and transdifferentiating plasmatocytes (P1$^+$ NRE$^+$) (Fig. 1B). As predicted, the vast majority (circa 80%) of the cortical zone is populated by plasmatocytes and, in accordance with the model, a double-positive population is comparatively small (Fig. 1B). Another, independent, criterion to further establish the qualitative differences between these three populations is cell size—a strong predictor of cell type in this system (Shrestha and Gateff, 1982; Leitão and Sucena, 2015). Indeed, cell size was found to differ significantly between cell populations (one-way ANOVA, $F = 173.3$, $P < 0.01$), with single P1$^+$ cells being the smallest and single NRE$^+$ the largest (Tukey HSD, diff = 21.89, $P < 0.01$); more importantly, the transdifferentiating cells show a distinct and intermediate size range (Tukey HSD, single P1$^+$ vs P1$^+$NRE$^+$, diff = 13.96, $P < 0.01$ and single NRE$^+$ vs P1$^+$NRE$^+$, diff = 7.93, $P < 0.01$) (Fig. 1C).

Having confirmed the existence of a Notch-activated transient stage, we proceeded to test if intermediate-stage cells, simultaneously expressing crystal cells and plasmatocytes terminal differentiation markers, could be observed. We stained lymph glands expressing a GFP-tagged Lozenge protein, a marker of committed crystal cells (Lebestky et al, 2000), with P1 antibody. As predicted, we observed a population of cells expressing both markers (Fig. 2A,a′). This result was further corroborated using Black-cell (BcF6-GFP), an earlier crystal cell marker that partially reproduces the endogenous pattern of the prophenoloxidase gene, PPO1 (Gajewski et al, 2007) and a Lozenge driver that mimics crystal cell expression of this transcription factor (Terriente-Felix et al, 2013) (Fig. EV1B–b',C–c').

We tested this hypothesis further by assessing whether crystal cells would descend from cortical plasmatocytes. Though expectedly rare, a transitional state consisting of triple-positive cells for plasmatocyte, Notch activation and crystal cell markers should exist within the cortical zone of third-instar lymph glands undergoing transdifferentiation. To explore this possibility, we used a BcF6-GFP reporter (Gajewski et al, 2007) that is activated by Lz. In hemizygous flies for the null allele LzS that lack crystal cells and phenoloxidase activity (Rizki and Rizki, 1981), this reporter will not be expressed but will display an expression pattern comparable to that of the endogenous PPO1 gene in flies wild-type for Lozenge function (Tokusumi et al, 2009). We crossed the BcF6-GFP crystal cell marker to a 12xSu(H)-LacZ Notch activation reporter (Go et al, 1998; Duvic et al, 2002) and stained the lymph glands with anti-P1.
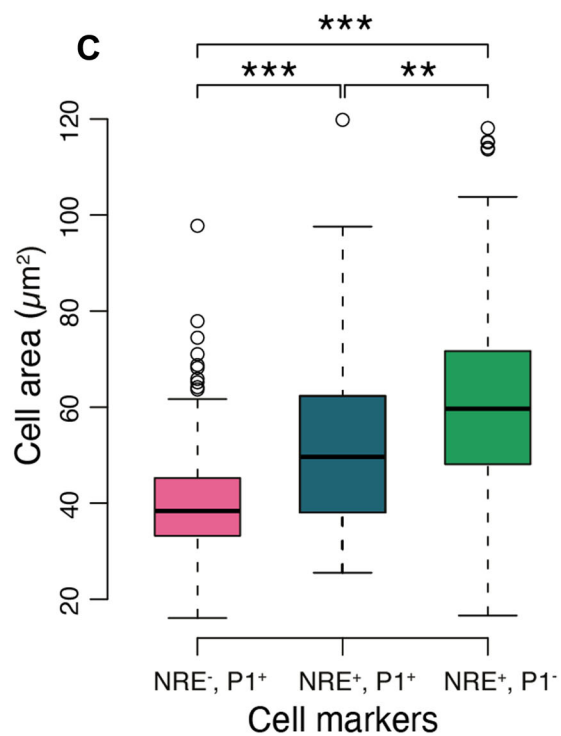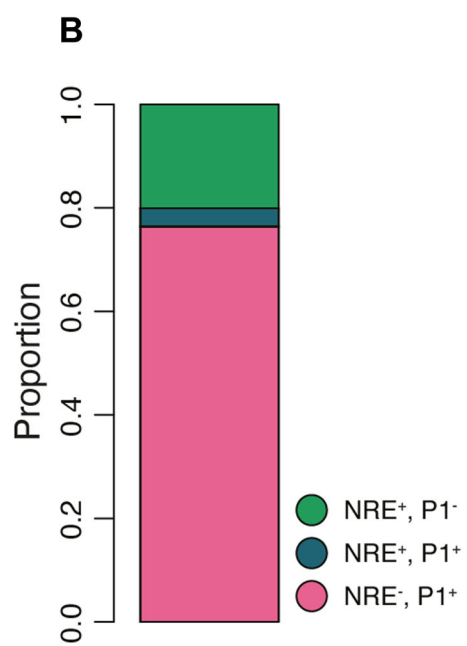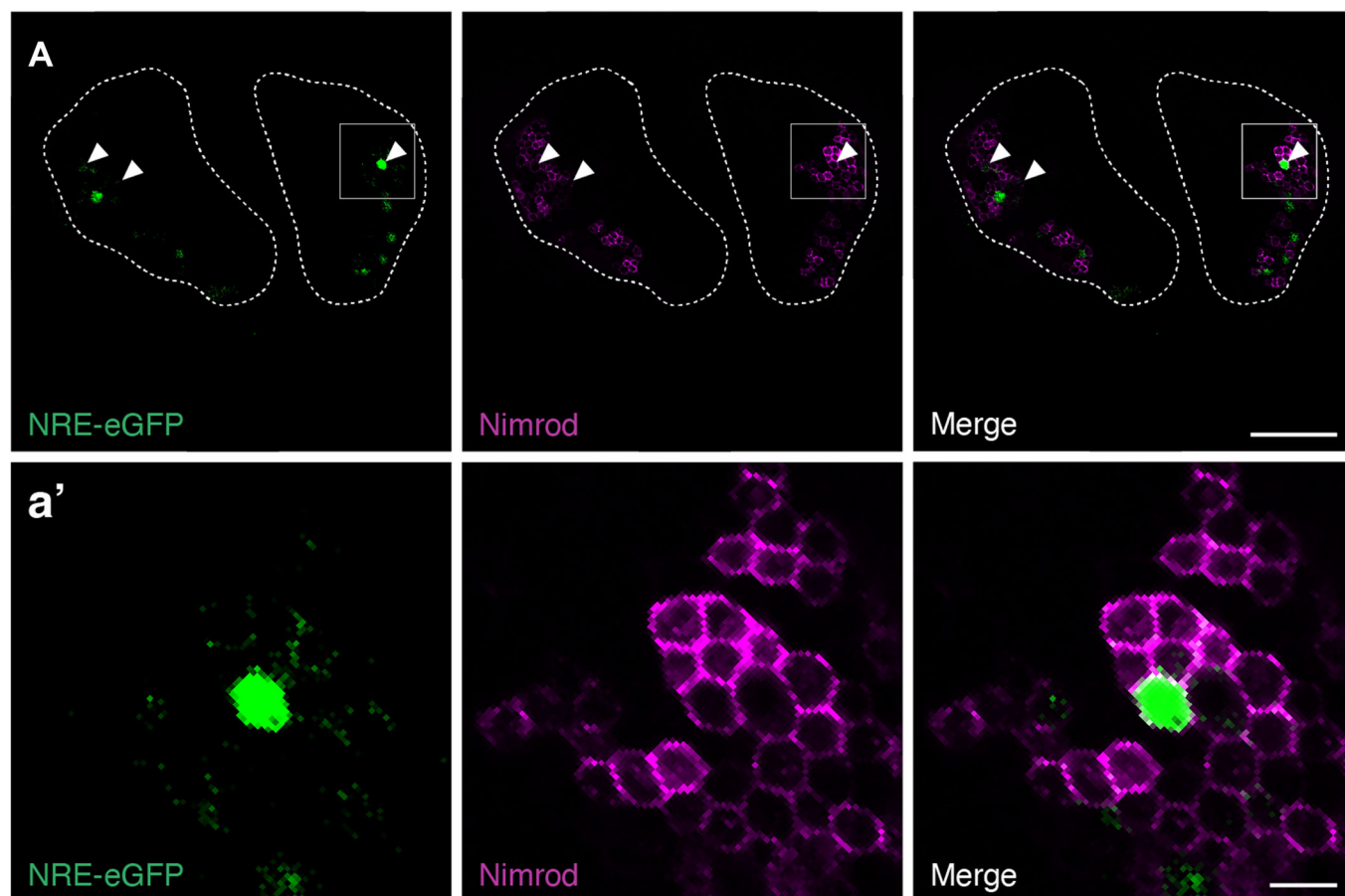
Figure 1. Notch signaling mediates transdifferentiation of cortical plasmatocytes into crystal cells.

(A) Lymph glands from larvae expressing the same NRE-eGFP notch activation reporter were stained with the anti-P1 antibody, a marker of mature plasmatocytes. We observe a population of mature plasmatocytes expressing GFP (white arrowheads), showing that there is a population of Notch-activated plasmatocytes in the cortical region of the lymph glands. Dotted lines define the contour of the primary lymph gland lobes. (a') Tenfold magnification of the inset shown in (A). (B) Quantification of the cells in (B) shows that the majority of marked cells (GFP and P1) are single positive plasmatocytes (76% single positive plasmatocytes), around 3.5% of the marked cells were positive for both markers and the remaining 20% are single GFP positive cells (presumably crystal cells). $n = 761$ cells from four lymph glands. (C) Quantification of the cell area showed a continuum in size from the smallest single P1-positive cells, through to the intermediate double positives and finally the largest single NRE-positive cells. This observation reaffirms the idea that the Notch-activated plasmatocytes are in the process of differentiating into crystal cells. Measurements of cell size were carried out manually by outlining cells in ImageJ at their largest area using Nimrod staining for plasmatocytes and cytoplasmic GFP for Notch activation. Although this is not the ideal, there is no cytoplasmic marker of mature plasmatocytes, and no membrane-localized notch activity reporter. Measuring cell areas using a cytoplasmic GFP will underestimate cell size, which should reduce the effect size observed. (NRE⁻,P1⁺ (582 cells): Min = 16.08, Q1 = 33.22, Median = 38.38, Q3 = 45.25, Max = 61.67; NRE⁺,P1⁺ (27 cells): Min = 25.51, Q1 = 38.09, Median = 49.63, Q3 = 63.30, Max = 97.59; NRE⁺,P1⁻ (153 cells): Min = 16.61, Q1 = 48.12, Median = 59.66, Q3 = 71.69, Max = 103.78). ***$P \le 0.001$, **$P \le 0.01$, *$P \le 0.05$. Cell areas were compared using a one-way ANOVA followed by Tukey's Honest Significant Difference method. The pairwise P values are as follows: NRE⁺,P1⁺ vs NRE⁻,P1⁺ $P = 0.0000003$; NRE⁺,P1⁻ vs NRE⁻,P1⁺ $P = 0.000000$; NRE⁺,P1⁻ vs NRE⁺,P1⁺ $P = 0.011504$. Scale bar represents 100 μm in (A), and 10 μm in (a'). Source data are available online for this figure.

The predicted triple-positive cells could be observed, providing additional validation of transdifferentiating cell presence (Fig. 2B,b').

Again, we could estimate the distribution of the three cell types and show that single positive plasmatocytes constitute circa 80% of the cells, the double-positive transdifferentiating cells are rare (3.3%), and single positive crystal cells account for the rest of the stained population within the cortical zone (Fig. 2C).

Lastly, if crystal cells would derive exclusively from medullary zone precursor cells, the total number of crystal cells should not be affected by Notch signaling blockage in cortical plasmatocytes. In contrast, the transdifferentiation model predicts a reduction of crystal cell numbers if Notch signaling is prevented within these differentiated plasmatocytes. To this aim, we knocked down *Notch* using RNAi driven by *eater*-GAL4, specifically interfering with a necessary crystal cell differentiation process within the plasmatocyte population. We observed a statistically significant reduction of crystal cells when reducing Notch levels relative to a control gene (Wilcox test, W = 10, P = 0.02) (Fig. 2D).

Taken together, the results above preclude us from rejecting a transdifferentiation process from plasmatocytes into crystal cells within the cortical zone of lymph glands of third-instar larvae.

Plasmatocyte-to-crystal cell transdifferentiation is a unidirectional process

Although consistent with our transdifferentiation model, the presence of cells transiently expressing both crystal cells and plasmatocytes-specific markers, in the lymph gland, is also compatible with the classic binary fate choice hypothesis. Under this scenario, markers of both cell types are expressed initially following which, one marker is lost, and cell fate is determined. This predicts that double-positive cells would give rise to both single-positive types. In contrast, the transdifferentiation model would predict that double positive cells will only give rise to crystal cells as they constitute an intermediate step in the directional process from plasmatocyte to crystal cell fate.

To test these alternative hypotheses, we performed two symmetrical G-TRACE lineage-tracing experiments, confined to the period from late L2 to late L3, using GAL80ts. The G-trace system permits the tracking of individual cells that have expressed or derive from cells which have expressed a particular driver (GAL4 line) during development. The expression of the driver, in this case,

is limited in time by the presence of a thermo-sensitive GAL80 allele (GAL80ts), that only permits GAL4 activity when the fly is placed at high temperatures. This drives a genomic rearrangement that maintains EGFP expression perpetually under the control of a ubiquitous promoter (Evans et al, 2009). First, we performed lineage-tracing with *eater*-GAL4, a driver expressed in cortical plasmatocytes (Tokusumi et al, 2009) coupled to UAS-FLP, Tub-GAL80ts and UbiFRTstopFRTStinger. In these flies, any cell and its progeny that has expressed *eater* (as mimicked by the *eater*-GAL4 driver line) will display green fluorescence. In addition, we performed antibody staining against Lozenge, a marker of crystal cells, on lymph glands dissected from these individuals. The presence of double-positive cells confirms that *eater*-expressing cells have become crystal cells (Fig. 3A). Complementarily, we did lineage-tracing by crossing an enhancer-trap Lz-Gal4 driver shown to be specific to crystal cells (Terriente-Felix et al, 2013) to UAS-FLP, Tub-GAL80ts, and UbiFRTstopFRTStinger, dissected lymph glands from the progeny and stained them with P1 antibody. In this case, any cell that has expressed Lozenge (crystal cell) will have green fluorescence perpetually and expression of P1 antigen (Nimrod) will indicate plasmatocyte identity. We could not observe double-positive cells in over 340 cells from 9 lymph glands (Fig. 3B). Unlike the previous experiment (Fig. 3A), where a class of double-positive cells could be observed, no cells that have expressed Lozenge (crystal cell fate) show a transition to plasmatocyte fate. Using eater-Gal4 UAS-dGFP (destabilized GFP), we confirmed the very low level of co-localization between a destabilized variant of GFP (dGFP) and Lozenge, revealed with anti-Lz immunostaining (~1.7%, Figs. EV2A,a',a'').

G-TRACE lineage-tracing experiments, although highly informative, do not provide a continuous time course for the process in study. To complement our lineage-tracing approach, we optimized a recently established protocol for lymph gland ex vivo culture (Ho et al, 2023), aiming to perform long-term imaging of lymph glands. For this purpose, late L3 larvae (120 h AEL) expressing, simultaneously, markers for plasmatocytes (Eater-dsRed) and crystal cells (BcF6-GFP) were used. In order to conduct the ex vivo assays, late L3 larvae were dissected, and the lymph gland complexes were cultured and imaged for 12 h, at 25 °C. In the end, we were able to image (single and randomly selected) primary lobes of 5 lymph glands, showing the exact moment where single positive Eater-DsRed cells (Eater-DsRed+ BcF6-GFP-) start to express BcF6-GFP, thus becoming double-positive cells (Eater-DsRed+
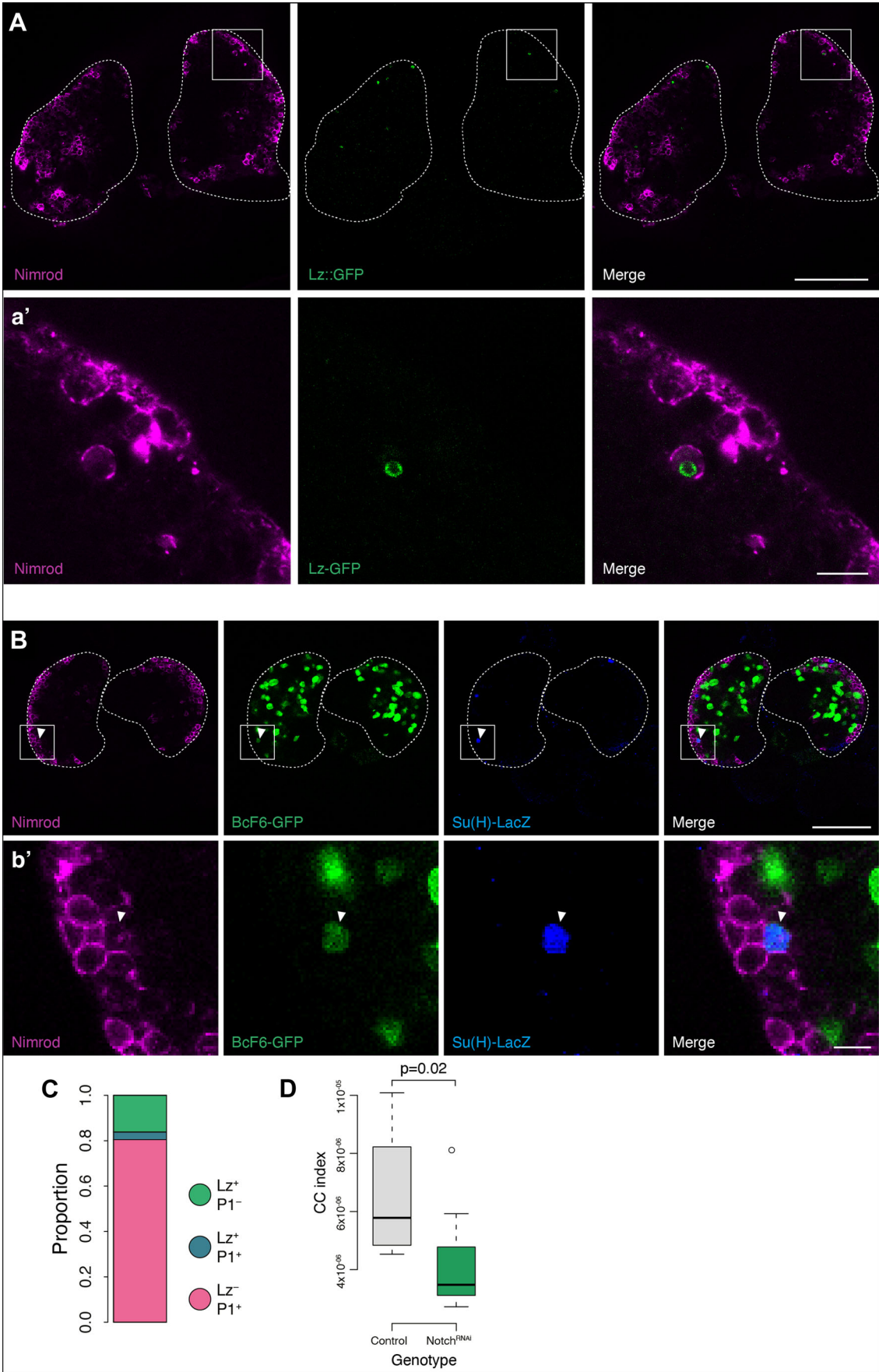
Figure 2. Notch signaling mediates transdifferentiation of cortical plasmatocytes into crystal cells.

(A) Lymph glands from larvae expressing a Lz-GFP fusion protein were stained with anti-P1, specific against the Nimrod protein. Cells were observed in the cortical zone expressing both proteins, consistently with the hypothesis that plasmatocytes are transdifferentiating into crystal cells. Dotted lines define the contour of the primary lymph gland lobes. (a′) Tenfold magnification of the inset in (A), showing an example of a double-positive Lz, P1 cell. (B) By combining a BcF6-GFP crystal cell marker with a 12xSu(H)-LacZ Notch activation reporter and staining the lymph glands with anti-P1 and Anti-βgal, we observed triple-positive cells (arrowheads). The existence of this population shows that some plasmatocytes activate the Notch pathway and initiate a crystal cell differentiation program. Dotted lines define the contour of the primary lymph gland lobes. (b′) Tenfold magnification of the inset in (B) showing an example of a BcF6-GFP + , Nimrod+ Su(H)-Lacz+ cell. (C) As in (A), 80% of cells are single positive for P1, 3% are double positive and 16% are single positive for Lz, reaffirming the transient nature of the transdifferentiating double-positive population. (D) Crystal cells differentiate from cortical plasmatocytes through a Notch-dependent mechanism. Crystal cell numbers are reduced when Notch is knocked down in the cortical differentiated plasmatocyte population (eater-GAL4 > UAS-NotchRNAi) compared to an unrelated RNAi control (eater-GAL4 > UAS-CG9313) (Control (8 lymph glands): Min = 4.52e-6, Q1 = 4.84e-06, Median = 5.78e-06, Q3 = 8.23e-06, Max = 1.01e-05; NotchRNAi (8 lymph glands): Min = 2.72e-06, Q1 = 3.11e-06, Median = 3.48e-06, Q3 = 4.78e-06, Max = 5.92e-06). Crystal cell numbers were normalized to lymph gland volume. CC indexes were compared using a Mann–Whitney U test. Scale bars in (A, B) represent 100 μm, and 10 μm in (a′, b′). Source data are available online for this figure.
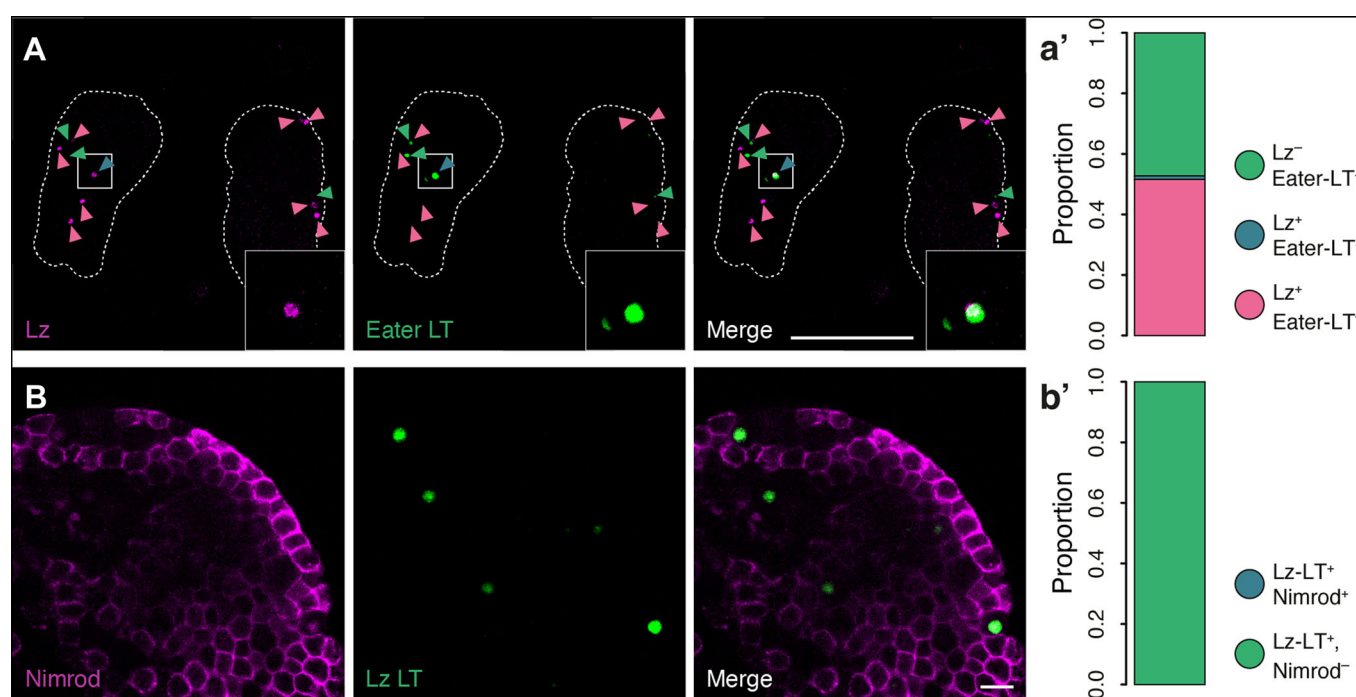

Figure 3. A unidirectional transdifferentiation program produces crystal cells from plasmatocytes.

(A) Lineage tracing of Eater-Gal4 followed by staining with anti-Lz. Double-positive cells are observed, indicating that some crystal cells originated from Eater-positive precursors. Magenta arrowheads mark Lz+ nuclei, green arrowhead mark cells lineage-traced for Eater-Gal4 but are Lz−, and cells indicated by blue arrowheads indicate cells positive for both (inside inset). Dotted lines define the contour of the primary lymph gland lobes. (a′) Quantification of the three cells types shown in (A). (B) By driving lineage tracing for Lz during larval development (limited with Tub-Gal80ts) and staining the lymph glands with anti-P1, lineage-traced cells were invariably negative for Nimrod (P1) (quantified in (b′)). This supports the idea that the double-positive cells do not revert back to plasmatocyte fate, and instead become crystal cells. (b′) Quantification of the three cells types shown in (B). Scale bars in (A) represent 100 μm and 10 μm in (B). Source data are available online for this figure.

BcF6-GFP +) (see Movie EV1). In accordance with the G-TRACE lineage-tracing experiments, no mature crystal cells (Eater-DsRed-BcF6-GFP +) were ever observed to become double positive. As such, we reinforce that these double-positive population likely represent cells undergoing unidirectional, plasmatocyte-to-crystal cell transdifferentiation. Due to technical difficulties, only four out of the five imaged lobes were quantifiable, for the proportion of cells within each of the three cell populations. Nonetheless, out of 1264 imaged cells, from 4 single lobes, belonging to 4 independent lymph glands: circa 96% of the cells were plasmatocytes, about 2.5% were crystal cells and only 1.5% were observed to become double-

positive, transdifferentiating cells—further attesting their rareness. Interestingly, at a point in time, some of these imaged double-positive cells momentarily acquired a "dark spot" within their BcF6-GFP expression domain. We speculate that these "spots" may be PPO crystals in production, which would reflect the functional switch between the two cell types (Fig. EV3).

Morphological analysis of these samples with segmented and tracked nuclei allowed us to determine where new crystal cells are differentiating in the lymph gland (Fig. EV4). We could confirm the presence of transdifferentiating cells within the outer 2 cell layers, a region that corresponds to the cortical zone. This observation is
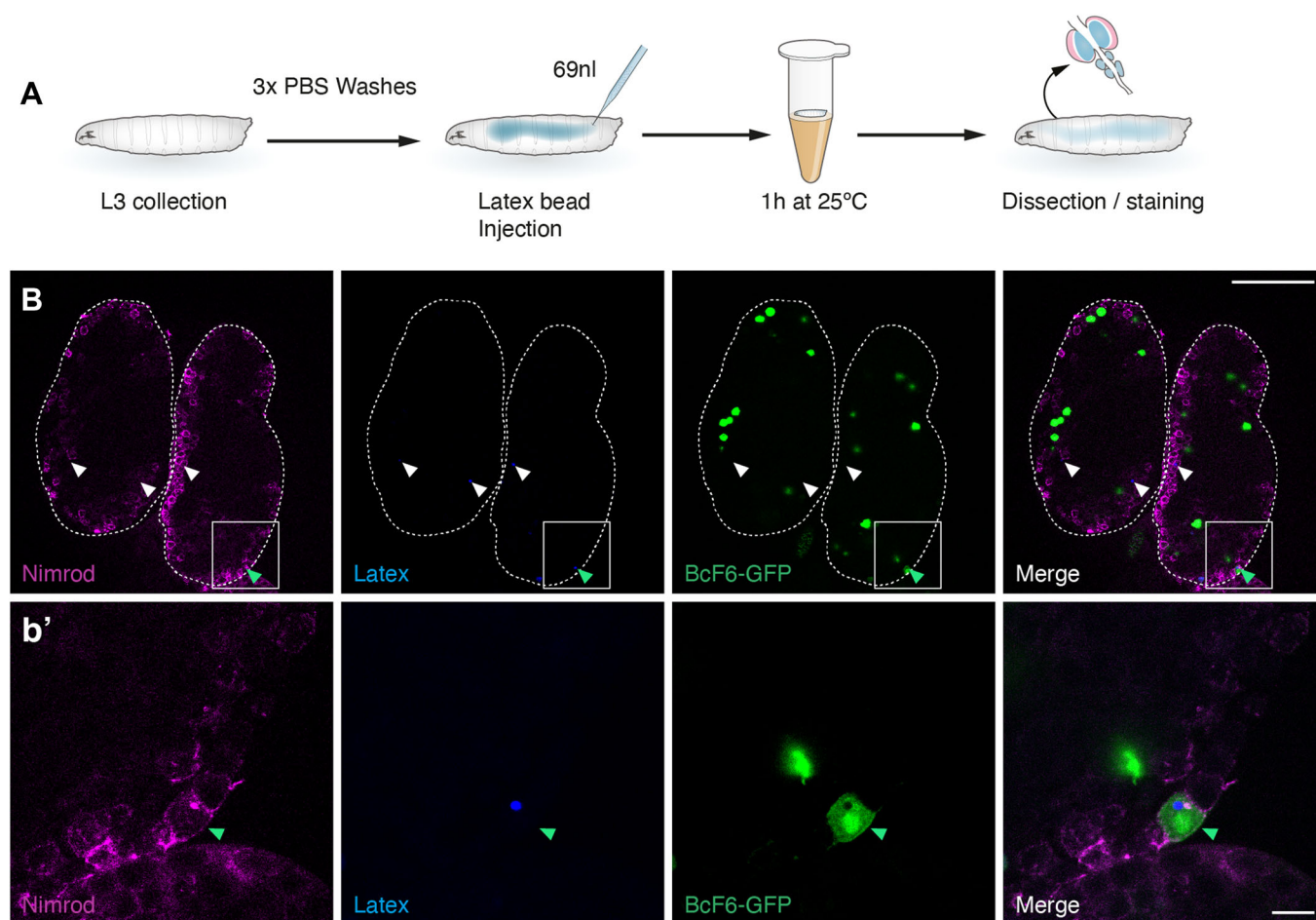
Figure 4. Cortical plasmatocytes are phagocytic cells that can transdifferentiate into crystal cells.

(A) Brief protocol of the in vivo phagocytosis assay. (B) We can detect fluorescent beads inside double-positive cells for P1 (plasmatocyte) and BcF6-GFP (crystal cell) (white and green arrowheads), confirming that active phagocytes can engage into a transdifferentiation process towards crystal cell fate. Dotted lines define the contour of the primary lymph gland lobes. (b') A zoomed region (inset) of (B) pointing with a green arrowhead a cell expressing Nimrod, BcF6-GFP and containing a phagocytosed latex bead (blue channel). Scale bar represents 100 μm in (B) and 10 μm in (b'). Source data are available online for this figure.

crucial because eater-dsRed, which uses the same enhancer as eater-GAL4, is expressed in distal progenitors of the intermediary zone (Blanco-Obregon et al, 2020). Consequently, our observations from the *Notch* knockdown experiment (Fig. 2D) and the analysis of *eater* lineage tracing (Fig. 3) could be explained by events occurring solely the distal part of the intermediary zone.

All of the above observations are consistent with a process in which mature plasmatocytes (P1-positive cells) activate the Notch pathway to initiate a crystal cell differentiation program consisting in the initiation of Lozenge and PPO1 expression, whilst shutting down plasmatocyte-specific genes such as Eater and Nimrod.

Transdifferentiating cells were once phagocytically active

We have shown that established bona fide markers of both plasmatocyte and crystal cell fate co-exist in the same cell population and confirmed the unidirectionality of the process. To complement these findings, we proceeded to test the functional transition from phagocytosis, the hallmark of fully differentiated

plasmatocytes, to a phenoloxidase-producing role. Our model predicts that some of these phagocytic cells will become crystal cells, transitioning from a Nimrod-positive to a Bc-positive state. To test this prediction, we performed in vivo and ex vivo phagocytic assays.

For the in vivo assay, blue fluorescent beads were injected into BcF6-GFP third-instar larvae (Fig. 4A)—similarly to an established protocol (Horn et al, 2014; preprint: Corcoran et al, 2020). The gene Bc (black cells) or PPO1 codes for prophenoloxidase 1, and is a marker of larval crystal cells (Rizki and Rizki, 1980a; Neyen et al, 2015). Dissected lymph glands at 1-h post-injection were stained with P1 antibody, allowing detection of both single positive populations and of the predicted double-positive population of transdifferentiating cells (Fig. 4B,b'). We observed beads inside plasmatocytes exclusively within the cortical region, as expected. More importantly, we could confirm the existence of double-positive cells containing beads (Fig. 4B,b'), providing qualitative evidence that a phagocytic cell, which has expressed plasmatocyte differentiation markers becomes a crystal cell. As a control and to assess the specificity of the phagocytic capacity, we mounted eye
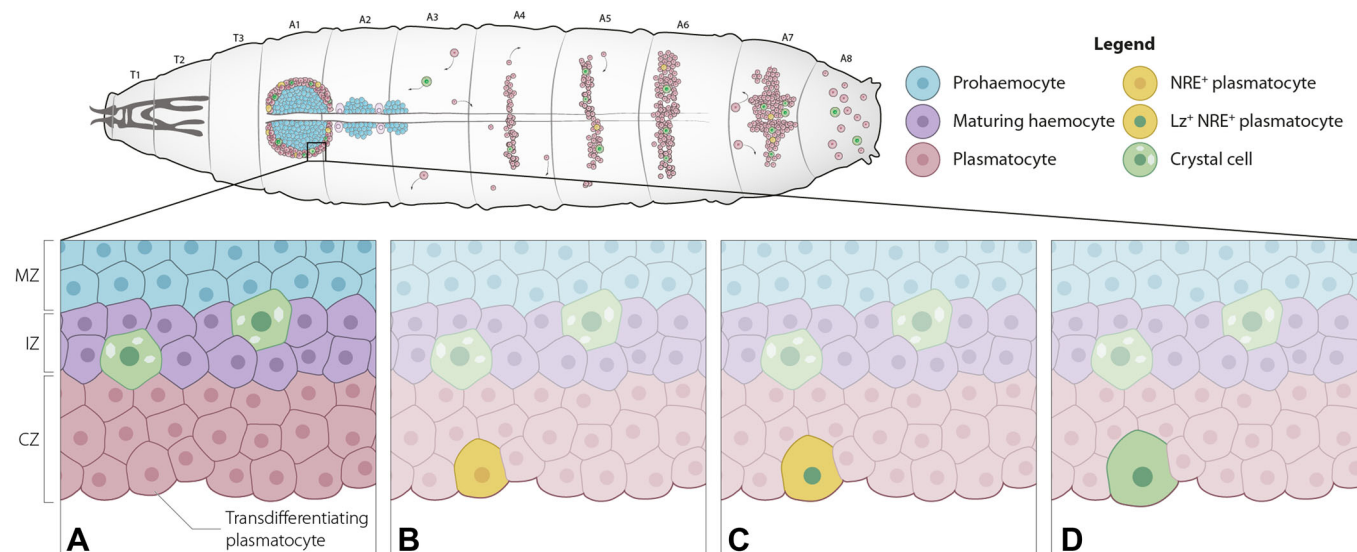
Figure 5. A model for crystal cell differentiation in the larval lymph gland.

Cortical plasmatocytes (red cells) derived from medullary prohaemocytes (blue cells) can engage in a Notch-dependent transdifferentiation process. A temporal notion of this process is provided in the succession of panels from (A) to (D), whereby Notch-activated plasmatocytes (yellow cells (B)) transiently express both cell type markers (yellow cell with green nucleus (C)), and become crystal cells (green cells (D)). These same cells and processes are shown in the clusters alluding to previously published data (Leitão and Sucena, 2015). Source data are available online for this figure.

discs which are surrounded by a patch of haemocytes (Holz et al, 2003). We can confirm that only haemocytes display internalized beads by comparison to the eye disc (ED) and optic lobe (OL) that do not contain beads (Fig. EV5).

As before, the presence of a double-positive population constitutes a qualitative criterion that precludes the rejection of the transdifferentiation model. Therefore, our observations corroborate further a mechanism through which crystal cells producing phenoloxidase may stem from the transdifferentiation of phagocytic Nimrod-positive cells.

Discussion

The overwhelmingly prevalent mode of crystal cell differentiation in the lymph gland is through a binary choice that occurs in immature haemocytes (progenitors), in a *Notch*-dependent manner (reviewed in Banerjee et al, 2019). However, in light of the evidence gathered here, we propose an additional mechanism for the production of crystal cells in the lymph gland of homeostatic larvae (Fig. 5). We posit that, as in the sessile clusters (Leitão and Sucena, 2015) and dorsal vessel (Cevik et al, 2019), crystal cells can be generated through the transdifferentiation of another functionally mature cell type, the plasmatocyte. This model is supported further by recent transcriptomics studies, showing crystal cell differentiation from haemocyte clusters expressing mature plasmatocyte markers, such as Eater and NimC1 (Cho et al, 2020; Girard et al, 2021; Hultmark and Andó 2022). During crystal cell differentiation, these markers are downregulated while mature crystal cell markers are upregulated (Cho et al, 2020; Girard et al, 2021). This mechanism parallels previously described transdifferentiation of plasmatocytes into crystal cells in the sessile haemocyte

clusters (Leitão and Sucena, 2015; preprint: Corcoran et al, 2020) and extends the established plasmatocyte transdifferentiation into lamellocytes within and outside the lymph gland (Honti et al, 2010; Anderl et al, 2016; Cho et al, 2020; Tattikota et al, 2020). Our observations—allied to these findings—support the occurrence of plasmatocyte-to-crystal cell transdifferentiation in the lymph gland, at multiple levels. Morphologically, we showed a transition in cell size throughout this process that matches the classical description of these cell types; functionally, lineage-tracing revealed the past phagocytic capacity of differentiating crystal cells, and through *ex vivo* long-term live imaging, the shift from plasmatocyte fate (shut-off) to crystal cell markers (activation). We argue that this transition from the expression of terminal markers of one cell type into another, concurrent with radical morphological and functional changes, support a transdifferentiation process rather than a classification of such cells as oligopotent.

Other important parallels have been established previously, namely the dependence on Notch/Serrate signaling for crystal cell differentiation in diverse contexts (Duvic et al, 2002; Lebestky et al, 2003; Leitão and Sucena, 2015; Cevik et al, 2019; Blanco-Obregon et al, 2020). Using a Serrate protein trap line (Nagarkar-Jaiswal et al, 2015), our observation of Serrate expression predominantly in the most external part of the cortical region, suggests this mechanism operates in the outer layer of the lymph gland (Fig. EV6). This outer layer is composed of mature cells (Jung et al, 2005; Crozatier and Meister, 2007), mostly plasmatocytes. Our data are consistent with this idea as shown by confined expression of markers for both plasmatocytes and crystal cells as well as for Notch pathway activation (Figs. 1, 2, and EV1). In brief, we argue that, for both the sessile clusters and the lymph gland, the Notch/Serrate pathway acts in interacting plasmatocytes to promote their transdifferentiation into crystal cells.

With the establishment of live imaging methods in the lymph gland, future studies may focus on the quantification of the duration of the transition state (double-positive cells). Despite not being able to observe the moment in which Eater-dsRed expression is "shut-down" in our experiments, we argue that Eater-dsRed might have been slow to denaturate in our setup, giving the impression of a longer duration of the transition state. Given the low proportion of the double-positive cell type in the overall haemocyte population (Figs. 1B, 2C, and 4), we predict that the transition state is likely to be a very fast process.

We interpret the higher proportion of crystal cells than expected (circa 20%) as a result of an under-estimation of plasmatocyte number, given that P1 is a late plasmatocyte marker and therefore provides a conservative estimate of plasmatocyte numbers. Indeed, plasmatocytes could be differentiated and active before strong and consistent expression of Nimrod and transdifferentiate before the detection of P1.

The parallels drawn here, between both haematopoietic contexts, may permit blood cell fate decisions to be addressed in the tractable sessile clusters and later validated in the lymph gland. Indeed, the generalization of a transdifferentiation mechanism across hematopoietic larval organs/tissues requires additional mechanistic evidence. Coupling the advances in in vivo imaging with the recent scRNA-seq studies of the lymph gland that have significantly advanced our understanding of blood cell differentiation (Cho et al, 2020; Tattikota et al, 2020; Girard et al, 2021), points the way to further studies. However, it is worth noticing that a considerable disparity in resolution remains between the subpopulations identified in scRNA-seq data and those marked by GAL4 drivers in the lymph gland. Hence, to validate the developmental pathways proposed in these studies, it is essential to develop new drivers that specifically target distinct blood cell subpopulations, which may require combinatorial strategies, such as the split-GAL4 system (Luan et al, 2006). This strategy may be applied to questions about the dynamics of cell differentiation over time and space, where live imaging is essential. For example, in the clusters the rate of import/export defines their size and the concomitant number of crystal cells, a seemingly central mechanism to the regulation of blood cell proportions (Leitão and Sucena, 2015). We speculate on an equivalence between the rate of crystal cell differentiation in the lymph gland as a function of the rate of plasmatocyte export to the cortical zone, and the rate of adhesion of circulating haemocytes to the sub-epidermal sessile clusters.

Notwithstanding the prevalence of binary switch mechanisms in cell fate decision (Cho et al, 2020), including in the lymph gland (Lebestky et al, 2000; Duvic et al, 2002; Banerjee et al, 2019), our findings may constitute an additional layer to this well-established canonical differentiation process. Importantly, these findings add to the transdifferentiation from plasmatocytes to crystal cells described in sessile clusters and the dorsal vessel (Leitão and Sucena, 2015; Cevik et al, 2019; preprint: Corcoran et al, 2020) supporting the generality of this mechanism in Drosophila larvae. Regardless of the size of the contribution transdifferentiation may have in normal lymph gland development and homeostatic conditions, the importance it may play if such conditions are under challenge, remains to be determined. Interestingly, two recent studies have shown that oxygen sensing may be at play, in promoting crystal cell differentiation in the lymph gland

(Mukherjee et al, 2011; Cho et al, 2018; Shin et al, 2024). As the role of oxygen sensing in promoting plasmatocyte-to-crystal cell transdifferentiation has already been shown in the sessile clusters surrounding the caudal sensory cones (preprint: Corcoran et al, 2020), it is possible that the same could happen in the context of the lymph gland. In addition, in the absence of PPO2, larvae display a physiological state of hypoxia even under normoxic conditions as this product of crystal cells fails to ensure its role in haemocyte guidance and systemic oxygen circulation (Shin et al, 2024). In this light, it will be interesting to re-visit the relative weight of transdifferentiation under hypoxic conditions, and whether this mechanism may be called upon with higher prevalence under stress. Future inquiries will determine whether transdifferentiation of plasmatocytes into crystal cells is a general mechanism, under local or systemic stress, to increase the deployment and response capacity of these cells (Binggeli et al, 2014; Dudzic et al, 2015; Vlisidou and Wood, 2015; Letourneau et al, 2016; Cho et al, 2018; Ramesh et al, 2021). Such future enquiry holds the promise of extending fundamental knowledge, gathered over more than half a century, on crystal cell differentiation and function in response to external aggression to promote melanization and wound-healing (Rizki, 1959; Rizki, and Rizki, 1980b; De Gregorio et al, 2002; Sorrentino, et al, 2002; Bidla et al, 2007; Eleftherianos and Revenis 2010; Dudzic et al, 2015; Banerjee et al, 2019; Shin et al, 2024).

As haematopoiesis in the Drosophila adult remains contentious, even after infection (Ghosh et al, 2015; Sanchez Bosch et al, 2019; Boulet et al, 2021), another aspect unaddressed is whether transdifferentiation occurs at this stage. The existence of such a mechanism could ensure plasticity in the regulation of haemocyte-type availability in the adult. Finally, a question remains on how these two processes may interplay and be modulated under different immunological and/or metabolic conditions (Ramond et al, 2020; Tiwari et al, 2020).

Transdifferentiation is gaining momentum, particularly in the context of development, regeneration, disease, and homeostatic balance (Slack, 2007; Thorel et al, 2010; Richard et al, 2011; Goldman, 2014; Defourny et al, 2015; Merrell and Stanger, 2016; Schaub et al, 2018; Wei et al, 2020). Albeit most reported cases involve cell division, a few exceptions have reported direct transdifferentiation, as described in our system (Beresford, 1990; Thorel et al, 2010; Jopling et al, 2011; Wei et al, 2020). Indeed, the reported switch from plasmatocyte to crystal cell fate in the lymph gland and in the sessile clusters obeys the three criteria postulated for this mechanism (Beresford, 1990): (i) cells are functionally mature, (ii) they change phenotype and, (iii) do not divide before transdifferentiating. In highly spatially structured systems such as the haematopoietic system of both Drosophila and vertebrates, particularly in its post-natal dimension, transdifferentiation may play a more prevalent role than previously appreciated. Finally, the generality of the transdifferentiation mechanisms in this system is of potential relevance to further develop genetic models of the vertebrate hematopoietic lineages (Crozatier and Vincent, 2011; Gold and Brückner, 2015; Banerjee et al, 2019), known to be highly context-dependent and plastic (Xie et al, 2004; Zhou et al, 2009; Sica and Mantovani, 2012; Hori, 2014; Dzierzak and Bigas, 2018) as well as for the study of regeneration and pathology (Slack, 2007; Jopling et al, 2011; Goldman, 2014; Zhou et al, 2014; Tanabe et al, 2018; Mollinari et al, 2018; Wei et al, 2020).

Methods

Reagents and tools table

Reagent/resource	Reference or source	Identifier or catalog number
Experimental models		
Drosophila Outbred population	Faria and Sucena, 2017	
HmlΔ-cytoDsRed	Clark et al, 2011	
BcF6-GFP	Gajewski et al, 2007	
Eater-Gal4	Tokusumi et al, 2009	
w; Eater-dsRed; BcF6-GFP		
12xSu(H)-LacZ		
HmlΔ-Gal4	Bloomington Drosophila Stock Center	BL-6395 and BL-6396
Lz-Gal4,UAS-GFP	Bloomington Drosophila Stock Center	BL-6313
NRE-eGFP	Bloomington Drosophila Stock Center	BL-30727
Lz-GFP.FPTB/TM6b	Bloomington Drosophila Stock Center	BL-43954
Ser-eGFP	Bloomington Drosophila Stock Center	BL-42314
w; Tub-Gal80ts; UAS-FLP, UbiFRTstopFRTStinger	Bloomington Drosophila Stock Center	BL-28282
UAS-NotchRNAi	Vienna Drosophila Stock Center	KK100002
UAS-SerRNAi	Vienna Drosophila Stock Center	KK108348
UAS-CG9313RNAi	Vienna Drosophila Stock Center	KK 103600
Antibodies		
Anti-Lozenge (Mouse)	DSHB	AB528346
Anti-NimrodC1 (Mouse)	Istvan Andó, Institute of Genetics, Szeged, Hungary	P1 antibody
Anti-GFP (Rabbit)	Torrey Pines Biolabs	TP401
Anti-βgal (Rabbit)	ThermoFisher	A-11132.
Anti-Mouse Alexa fluor 488	Invitrogen	A-11001
Anti-Mouse Alexa fluor 546	Invitrogen	A-11008
Anti-Rabbit Alexa fluor 488	Invitrogen	A-11001
Anti-Rabbit Alexa fluor Cy5	Invitrogen	A-10523
Other		
Amine-modifiedpolystyrene, fluorescent blue Latex beads	Sigma-Aldrich	L0280

Stock maintenance

Flies were kept under room temperature and fed with a standard cornmeal-agar medium, consisting of 4.5% molasses, 7.5% sugar, 7% corn-flower, 2% granulated yeast extract, 1% agar and 0.25% nipagin, mixed in distilled water. Experiments were carried out at 25 °C, apart from the lineage tracing in which egg lays were kept at 18 °C during the restrictive phase and moved to the permissive 29 °C at 44 h after egg lay. For RNAi experiments, egg lays were carried out at 25 °C following which the eggs were moved to 29 °C. For experiments with the Lz-GFP.FPTB/TM6b, we outcrossed the stock and selected non-tubby larvae for observation.

Fly stocks

The following fly stocks were used: Drosophila Outbred population (Faria and Sucena, 2017), HmlΔ-cytoDsRed (Clark et al, 2011) (a gift from Marc Dionne), BcF6-GFP (Gajewski et al, 2007) and Eater-Gal4 (Tokusumi et al, 2009), w; Eater-dsRed; BcF6-GFP (a gift from Robert A. Shultz); from the Bloomington stock center: HmlΔ-Gal4 (BL-6395 and BL-6396), Lz-Gal4 was derived from Lz-Gal4, UAS-GFP (BL-6313) (Crew et al, 1997), NRE-eGFP (Saj et al, 2010) (BL-30727), 12xSu(H)-LacZ (Go et al, 1998), Lz-GFP.FPTB/TM6b (BL-43954), Ser-eGFP (Nagarkar-Jaiswal et al, 2015) (BL-42314); from the VDRC stock center: UAS-NotchRNAi (KK100002), UAS-SerRNAi (KK108348) and UAS-CG9313RNAi (KK 103600). To carry out temperature-dependent lineage tracing, females of w; Tub-Gal80ts; UAS-FLP, UbiFRTstopFRTStinger (from Bloomington stock BL-28282) were crossed with males from the Lz-Gal4 driver at 18 °C. Only females were analyzed.

Immunostaining

Lymph gland dissections and immunostaining were carried out following the protocols described by (Evans et al, 2014). Briefly, for all experiments, wandering stage L3 larvae (120 h AEL) were washed 3× in 1×PBS to remove yeast from the cuticle. Larvae were dissected in cold PBS and the lymph glands transferred with the mouth hooks and brain complex to 1 ml of 0.002% ice-cold PBST× (Evans et al, 2014). After 30 min of dissection, the lymph glands were fixed in 3.7% formaldehyde. After 3 × 15-min washes in 0.4× PBST×, the lymph glands were blocked in 5x blocking buffer (5×NDS in 0.4×PBST×), and subsequently incubated in primary antibodies diluted in blocking buffer. Both the primary and secondary antibody incubations were carried out overnight at 4 °C.

The following primary antibodies were used in the following concentrations:

1:100 Anti-P1 (Mouse), 1:500 Anti-GFP (Rabbit), 1:200 Anti-βgal (Rabbit), 1:100 Anti-Lz (Mouse).

The following secondary antibodies were used in the indicated dilutions:

Anti-Mouse af488 (1:250), Anti-Mouse af546 (1:250), Anti-Rabbit af488 (1:500), Anti-Rabbit afCy5 (1:250).

Samples were mounted in Vectashield then imaged using a Leica SP5 confocal using either a ×40 dry, ×40 oil immersion or ×20 dry objectives. Image processing and quantification were carried out in Fiji (Schindelin et al, 2012) with the Bio-Formats plugin (Linkert et al, 2010).

Ex vivo lymph gland long-term imaging

Lymph gland dissections, culturing and imaging were carried out following the protocols described by (Ho et al, 2023). Briefly, fate third-instar larvae (200 AEL), from a *w; Eater-dsRed; BcF6-GFP* line, were selected and washed, then dissected in in Drosophila Schneider's medium at room temperature. The connection between target organs—including larval lymph gland, fat bodies, central nervous system and

heart tube - was maintained during all steps—from dissection, to mounting and imaging—for structural integrity purposes. The dissected organ complexes were mounted in a glass bottom dish with PBS, over a 0.1% L-polylysine coat, and cultured in Schneider's medium supplied with 15% FBS (ThermoFisher Scientific, #12483-020) and 0.2 mg/mL insulin (Sigma I0516); the culture medium was prepared fresh, 10 min prior to dissection. The organ-complex was then covered with a 1% agar pad, and 2 ml of the medium, in order to maintain optimal moisture conditions during live imaging. All live imaging experiments were performed for 12 h, at 25 °C, using an LSM980+Airyscan inverted light sheet microscope, with a ×40 water immersion lens. The obtained lymph gland z-sections were spaced by 1 μm, and imaged at a 5- (first movie obtained) or 10-minute (remaining 4 movies obtained) intervals, using excitation at 488 nm (green laser) and 561 nm (red laser). Time-lapse recordings of lymph glands, and resulting t-series images, were processed using Fiji (Schindelin et al, 2012) and IMARIS (Oxford Instruments) to segment and track nuclei over time.

In vivo phagocytic assays

L3 larvae from a BcF6-GFP line introgressed into an outbred background were collected and washed 3× in 1×PBS. 2 μm of blue fluorescent latex beads (Sigma-Aldrich) were diluted 1:10 in 1×PBS and 69 nl of the suspension was injected into the posterior of the larva at 230 nl/second using a microinjector (Drummond Nanoject II Auto-Nanoliter Injector). The larvae were transferred to food and incubated for 1 h at 25 °C, after which they were collected, their lymph glands dissected and stained with Anti-P1 (as above).

Statistical analysis

Statistics and graphics were produced in R (version 3.3.0) (R Core Team, 2016). ANOVA followed by Tukey's HSD post-hoc test was used to compare the cell areas of the NRE and Nimrod-positive populations. Wilcox test was used to compare the crystal cell index in the Notch knockdown experiment.

Data availability

Source data is available at: https://drive.google.com/drive/folders/1pKtjfpmczLmOZSxcf2kKnKum-0-XGqPq?usp=sharing.

The source data of this paper are collected in the following database record: biostudies:S-SCDT-10_1038-S44319-025-00366-z.

Expanded view data, supplementary information, appendices are available for this paper at https://doi.org/10.1038/s44319-025-00366-z.

Peer review information

A peer review file is available at https://doi.org/10.1038/s44319-025-00366-z

References

Anderl I, Vesala L, Ihalainen TO, Vanha-aho LM, Andó I, Rämet M, Hultmark D (2016) Transdifferentiation and proliferation in two distinct hemocyte lineages in Drosophila melanogaster larvae after wasp infection. PLoS Pathog 12:e1005746. https://doi.org/10.1371/journal.ppat.1005746

Banerjee U, Girard JR, Goins LM, Spratford CM (2019) Drosophila as a genetic model for hematopoiesis. Genetics 211:367–417. https://doi.org/10.1534/genetics.118.300223

Beresford WA (1990) Direct transdifferentiation: can cells change their phenotype without dividing? Cell Differ Dev 29:81–93. https://doi.org/10.1016/0922-3371(90)90026-S

Bidla G, Dushay MS, Theopold U (2007) Crystal cell rupture after injury in Drosophila requires the JNK pathway, small GTPases and the TNF homolog Eiger. J Cell Sci 120(Pt 7):1209–1215. https://doi.org/10.1242/jcs.03420

Binggeli O, Neyen C, Poidevin M, Lemaitre B (2014) Prophenoloxidase activation is required for survival to microbial infections in Drosophila. PLoS Pathog 10(5):e1004067. https://doi.org/10.1371/journal.ppat.1004067

Blanco-Obregon D, Katz MJ, Durrieu L, Gándara L, Wappner P (2020) Context-specific functions of Notch in Drosophila blood cell progenitors. Dev Biol 462:101–115. https://doi.org/10.1016/j.ydbio.2020.03.018

Boulet M, Renaud Y, Lapraz F, Benmimoun B, Vandel L, Waltzer L (2021) Characterization of the Drosophila adult hematopoietic system reveals a rare cell population with differentiation and proliferation potential. Front Cell Dev Biol 9:739357. https://doi.org/10.3389/fcell.2021.739357

Bretscher AJ, Honti V, Binggeli O, Burri O, Poidevin M, Kurucz E, Zsámboki A, Andó I, Lemaitre B (2015) The Nimrod transmembrane receptor Eater is required for hemocyte attachment to the sessile compartment in Drosophila melanogaster. Biol Open 4:355–363. https://doi.org/10.1242/bio.201410595

Brooks EC, Zeidler MP, Ong ACM, Evans IR (2024) Macrophage subpopulation identity in Drosophila is modulated by apoptotic cell clearance and related signalling pathways. Front Immunol 14:1310117. https://doi.org/10.3389/fimmu.2023.1310117

Cattenoz PB, Sakr R, Pavlidaki A, Delaporte C, Riba A, Molina N, Hariharan N, Mukherjee T, A Giangrande (2020) Temporal specificity and heterogeneity of Drosophila immune cells. EMBO J. https://doi.org/10.15252/embj.2020104486.

Cevik D, Acker M, Michalski C, Jacobs JR (2019) Pericardin, a Drosophila collagen, facilitates accumulation of hemocytes at the heart. Dev Biol 454:52–65. https://doi.org/10.1016/j.ydbio.2019.06.006

Cho B, Spratford CM, Yoon S, Cha N, Banerjee U, Shim J (2018) Systemic control of immune cell development by integrated carbon dioxide and hypoxia chemosensation in Drosophila. Nat Commun 9:2679. https://doi.org/10.1038/s41467-018-04990-3

Cho B, Yoon SH, Lee D, Koranteng F, Tattikota SG, Cha N, Shin M, Do H, Hu Y, Young Oh S et al (2020) Single-cell transcriptome maps of myeloid blood cell lineages in Drosophila. Nat Commun 11:4483. https://doi.org/10.1038/s41467-020-18135-y

Clark RI, Woodcock KJ, Geissmann F, Trouillet C, Dionne MS (2011) Multiple TGF-β superfamily signals modulate the adult Drosophila immune response. Curr Biol 21:1672–1677. https://doi.org/10.1016/j.cub.2011.08.048

Coates JA, Brooks E, Brittle AL, Armitage EL, Zeidler MP, Evans IR (2021) Identification of functionally distinct macrophage subpopulations in Drosophila. eLife 10:e58686. https://doi.org/10.7554/eLife.58686

Corcoran S, Mase A, Hashmi Y, Ouyang D, Augsburger J, Jacobs T, Kukar K, Brückner K (2020) Regulation of blood cell transdifferentiation by oxygen sensing neurons. Preprint at bioRxiv https://doi.org/10.1101/2020.04.22.056622

Crew JR, Batterham P, Pollock JA (1997) Developing compound eye in lozenge mutants of Drosophila: lozenge expression in the R7 equivalence group. Dev Genes Evol 206:481–493. https://doi.org/10.1007/s004270050079

Crozatier M, Meister M (2007) Drosophila haematopoiesis. Cell Microbiol 9:1117–1126. https://doi.org/10.1111/j.1462-5822.2007.00930.x

Crozatier M, Vincent A (2011) *Drosophila*: a model for studying genetic and molecular aspects of haematopoiesis and associated leukaemias. Dis Models Mechan 4:439–445. https://doi.org/10.1242/dmm.007351

Csordás G, Gábor E, Honti V (2021) There and back again: the mechanisms of differentiation and transdifferentiation in Drosophila blood cells. Dev Biol 469:135–143. https://doi.org/10.1016/j.ydbio.2020.10.006

De Gregorio E, Han S-J, Lee W-J, Baek MJ, Osaki T, Kawabata SI, Lee B-L, Iwanaga S, Lemaitre B, Brey PT (2002) An immune-responsive Serpin regulates the melanization cascade in Drosophila. Dev Cell 3(4):581–592. https://doi.org/10.1016/s1534-5807(02)00267-8

Defourny J, Mateo Sánchez S, Schoonaert L, Robberecht W, Davy A, Nguyen L, Malgrange B (2015) Cochlear supporting cell transdifferentiation and integration into hair cell layers by inhibition of ephrin-B2 signalling. Nat Commun 6:7017. https://doi.org/10.1038/ncomms8017

Dudzic JP, Kondo S, Ueda E, Bergman CM, Lemaitre B (2015) Drosophila innate immunity: regional and functional specialization of prophenoloxidases. BMC Biol 13:81. https://doi.org/10.1186/s12915-015-0193-6

Duvic B, Hoffmann JA, Meister M, Royet J (2002) Notch signaling controls lineage specification during *Drosophila* larval hematopoiesis. Curr Biol 12:1923–1927. https://doi.org/10.1016/s0960-9822(02)01297-6

Dzierzak E, Bigas A (2018) Blood development: hematopoietic stem cell dependence and independence. Cell Stem Cell 22:639–651. https://doi.org/10.1016/j.stem.2018.04.015

Eleftherianos I, Revenis C (2010) Role and importance of phenoloxidase in insect hemostasis. J Innate Immun 3(1):28–33. https://doi.org/10.1159/000321931

Evans CJ, Hartenstein V, Banerjee U (2003) Thicker than blood: conserved mechanisms in *Drosophila* and vertebrate hematopoiesis. Dev Cell 5:673–690. https://doi.org/10.1016/S1534-5807(03)00335-6

Evans CJ, Liu T, Banerjee U (2014) *Drosophila* hematopoiesis: markers and methods for molecular genetic analysis. Methods 68:242–251. https://doi.org/10.1016/j.ymeth.2014.02.038

Evans CJ, Olson JM, Ngo KT, Kim E, Lee NE, Kuoy E, Patananan AN, Sitz D, Tran PT, Do M-T et al (2009) G-TRACE: rapid Gal4-based cell lineage analysis in *Drosophila*. Nat Methods 6:603–605. https://doi.org/10.1038/nmeth.1356

Faria VG, Sucena É (2017) From nature to the lab: establishing *Drosophila* resources for evolutionary genetics. Front Ecol Evol. https://doi.org/10.3389/fevo.2017.00061

Ferguson GB, Martinez-Agosto JA (2014) Yorkie and scalloped signaling regulates Notch-dependent lineage specification during *Drosophila* hematopoiesis. Curr Biol 24:2665–2672. https://doi.org/10.1016/j.cub.2014.09.081

Fu Y (2020) Single-cell RNA sequencing identifies novel cell types in Drosophila blood. J Genet Genomics. https://doi.org/10.1016/j.jgg.2020.02.004

Gajewski KM, Sorrentino RP, Lee JH, Zhang Q, Russell M, Schulz RA (2007) Identification of a crystal cell-specific enhancer of the black cells prophenoloxidase gene in drosophila. Genesis 45:200–207. https://doi.org/10.1002/dvg.20285

Ghosh S, Singh A, Mandal S, Mandal L (2015) Active hematopoietic hubs in *Drosophila* adults generate hemocytes and contribute to immune response. Dev Cell 33:478–488. https://doi.org/10.1016/j.devcel.2015.03.014

Girard JR, Goins LM, Vuu DM, Sharpley MS, Spratford CM, Mantri SR, Banerjee U (2021) Paths and pathways that generate cell-type heterogeneity and developmental progression in hematopoiesis. eLife 10:e67516. https://doi.org/10.7554/eLife.67516

Go MJ, Eastman DS, Artavanis-Tsakonas S (1998) Cell proliferation control by Notch signaling in *Drosophila* development. Development 125:2031–2040. https://doi.org/10.1242/dev.125.11.2031

Gold KS, Brückner K (2015) Macrophages and cellular immunity in *Drosophila melanogaster*. Semin Immunol 27:357–368. https://doi.org/10.1016/j.smim.2016.03.010

Goldman D (2014) Müller glial cell reprogramming and retina regeneration. Nat Rev Neurosci 15:431–442. https://doi.org/10.1038/nrn3723

Grigorian M, Hartenstein V (2013) Hematopoiesis and hematopoietic organs in arthropods. Dev Genes Evol 223:103–115. https://doi.org/10.1007/s00427-012-0428-2

Ho KYL, Carr RL, Dvoskin AD, Tanentzapf G (2023) Kinetics of blood cell differentiation during hematopoiesis revealed by quantitative long-term live imaging. eLife 12:e84085. https://doi.org/10.7554/eLife.84085

Holz A, Bossinger B, Strasser T, Janning W, Klapper R (2003) The two origins of hemocytes in *Drosophila*. Development 130:4955–4962. https://doi.org/10.1242/dev.00702

Honti V, Csordás G, Márkus R, Kurucz É, Jankovics F, Andó I (2010) Cell lineage tracing reveals the plasticity of the hemocyte lineages and of the hematopoietic compartments in *Drosophila melanogaster*. Mol Immunol 47:1997–2004. https://doi.org/10.1016/j.molimm.2010.04.017

Hori S (2014) Lineage stability and phenotypic plasticity of $Foxp3^+$ regulatory T cells. Immunol Rev 259:159–172. https://doi.org/10.1111/imr.12175

Horn L, Leips J, Starz-Gaiano M (2014) Phagocytic ability declines with age in adult *Drosophila* hemocytes. Aging Cell 13:719–728. https://doi.org/10.1111/acel.12227

Hultmark D, Andó I (2022) Hematopoietic plasticity mapped in Drosophila and other insects. eLife 11:e78906. https://doi.org/10.7554/eLife.78906

Jopling C, Boue S, Izpisua Belmonte JC (2011) Dedifferentiation, transdifferentiation and reprogramming: three routes to regeneration. Nat Rev Mol Cell Biol 12:79–89. https://doi.org/10.1038/nrm3043

Jung S-H, Evans CJ, Uemura C, Banerjee U (2005) The *Drosophila* lymph gland as a developmental model of hematopoiesis. Development 132:2521–2533. https://doi.org/10.1242/dev.01837

Kharrat B, Csordás G, Honti V (2022) Peeling back the layers of lymph gland structure and regulation. Int J Mol Sci. https://doi.org/10.3390/ijms23147767

Kocks C, Cho JH, Nehme N, Ulvila J, Pearson AM, Meister M, Strom C, Conto SL, Hetru C, Stuart LM et al (2005) Eater, a transmembrane protein mediating phagocytosis of bacterial pathogens in *Drosophila*. Cell 123:335–346. https://doi.org/10.1016/j.cell.2005.08.034

Krzemien J, Crozatier M, Vincent A (2010a) Ontogeny of the *Drosophila* larval hematopoietic organ, hemocyte homeostasis and the dedicated cellular immune response to parasitism. Int J Dev Biol 54:1117–1125. https://doi.org/10.1387/ijdb.093053jk

Krzemien J, Oyallon J, Crozatier M, Vincent A (2010b) Hematopoietic progenitors and hemocyte lineages in the *Drosophila* lymph gland. Dev Biol 346:310–319. https://doi.org/10.1016/j.ydbio.2010.08.003

Kurucz É, Márkus R, Zsámboki J, Folkl-Medzihradszky K, Darula Z, Vilmos P, Udvardy A, Krausz I, Lukacsovich T, Gateff E et al (2007) Nimrod, a putative phagocytosis receptor with EGF repeats in *Drosophila* plasmatocytes. Curr Biol 17:649–654. https://doi.org/10.1016/j.cub.2007.02.041

Lai EC (2005) The ubiquitin ligase *Drosophila* Mind bomb promotes Notch signaling by regulating the localization and activity of serrate and delta. Development 132:2319–2332. https://doi.org/10.1242/dev.01825

Lanot R, Zachary D, Holder F, Meister M (2001) Postembryonic hematopoiesis in *Drosophila*. Dev Biol 230:243–257. https://doi.org/10.1006/dbio.2000.0123

Lebestky T, Chang T, Hartenstein V, Banerjee U (2000) Specification of *Drosophila* hematopoietic lineage by conserved transcription factors. Science 288:146–149. https://doi.org/10.1126/science.288.5463.146

Lebestky T, Jung S, Banerjee U (2003) A Serrate-expressing signaling center controls *Drosophila* hematopoiesis. Genes Dev 17:348–353. https://doi.org/10.1101/gad.1052803

Leitão AB, Arunkumar R, Day JP, Geldman EM, Morin-Poulard I, Crozatier M, Jiggins FM (2020) Constitutive activation of cellular immunity underlies the

evolution of resistance to infection in *Drosophila*. eLife 9:e59095. https://doi.org/10.7554/eLife.59095

Leitão AB, Sucena É (2015) *Drosophila* sessile hemocyte clusters are true hematopoietic tissues that regulate larval blood cell differentiation. eLife https://doi.org/10.7554/eLife.06166

Letourneau M, Lapraz F, Sharma A, Vanzo N, Waltzer L, Crozatier M (2016) *Drosophila* hematopoiesis under normal conditions and in response to immune stress. FEBS Lett 590:4034–4051. https://doi.org/10.1002/1873-3468.12327

Linkert M, Rueden CT, Allan C, Burel JM, Moore W, Patterson A, Loranger B, Moore J, Neves C, Macdonald D et al (2010) Metadata matters: access to image data in the real world. J Cell Biol 189:777–782. https://doi.org/10.1083/jcb.201004104

Luan H, Peabody NC, Vinson CR, White BH (2006) Refined spatial manipulation of neuronal function by combinatorial restriction of transgene expression. Neuron 52(3):425–436. https://doi.org/10.1016/j.neuron.2006.08.028

Makhijani K, Alexander B, Tanaka T, Rulifson E, Bruckner K (2011) The peripheral nervous system supports blood cell homing and survival in the *Drosophila* larva. Development 138:5379–5391. https://doi.org/10.1242/dev.067322

Márkus R, Laurinyecz B, Kurucz E, Honti V, Bajusz I, Sipos B, Somogyi K, Kronhamn J, Hultmark D, Andó I (2009) Sessile hemocytes as a hematopoietic compartment in *Drosophila melanogaster*. Proc Natl Acad Sci USA 106:4805–4809. https://doi.org/10.1073/pnas.0801766106

Merrell AJ, Stanger BZ (2016) Adult cell plasticity in vivo: de-differentiation and transdifferentiation are back in style. Nat Rev Mol Cell Biol 17:413–425. https://doi.org/10.1038/nrm.2016.24

Mollinari C, Zhao J, Lupacchini L, Garaci E, Merlo D, Pei G (2018) Transdifferentiation: a new promise for neurodegenerative diseases. Cell Death Dis. 9:1–9. https://doi.org/10.1038/s41419-018-0891-4

Mukherjee T, Kim WS, Mandal L, Banerjee U (2011) Interaction between Notch and Hif-alpha in development and survival of Drosophila blood cells. Science 332(6034):1210–1213. https://doi.org/10.1126/science.1199643

Nagarkar-Jaiswal S, Lee P-T, Campbell ME, Chen K, Anguiano-Zarate S, Cantu Gutierrez M, Busby T, Lin W-W, He Y, Schulze KL et al (2015) A library of MiMICs allows tagging of genes and reversible, spatial and temporal knockdown of proteins in *Drosophila*. eLife https://doi.org/10.7554/eLife.05338

Neyen C, Binggeli O, Roversi P, Bertin L, Sleiman MB, Lemaitre B (2015) The Black cells phenotype is caused by a point mutation in the *Drosophila* pro-phenoloxidase 1 gene that triggers melanization and hematopoietic defects1Equal contribution.1. Dev Comp Immunol 50:166–174. https://doi.org/10.1016/j.dci.2014.12.011

R Core Team (2016) R: a language and environment for statistical computing. Vienna, Austria: R Foundation for Statistical Computing. Available at: https://www.R-project.org/

Ramesh P, Dey NS, Kanwal A, Mandal S, Mandal L (2021) Relish plays a dynamic role in the niche to modulate *Drosophila* blood progenitor homeostasis in development and infection. eLife 10:e67158. https://doi.org/10.7554/eLife.67158

Ramond E, Dudzic JP, Lemaitre B (2020) Comparative RNA-Seq analyses of *Drosophila* plasmatocytes reveal gene specific signatures in response to clean injury and septic injury. PLoS ONE 15:e0235294. https://doi.org/10.1371/journal.pone.0235294

Richard JP, Zuryn S, Fischer N, Pavet V, Vaucamps N, Jarriault S (2011) Direct in vivo cellular reprogramming involves transition through discrete, non-pluripotent steps. Development 138:1483–1492. https://doi.org/10.1242/dev.063115

Rizki MTM (1957) Alterations in the haemocyte population of *Drosophila melanogaster*. J Morphol 100:437–458. https://doi.org/10.1002/jmor.1051000303

Rizki MTM (1959) Functional significance of the crystal cells in the larva of *Drosophila melanogaster*. J Biophys Biochem Cytol 5(2):235–240. https://doi.org/10.1083/jcb.5.2.235

Rizki TM, Rizki RM (1980a) Developmental analysis of a temperature-sensitive melanotic tumor mutant in *Drosophila melanogaster*. Wilhelm Roux's Arch Dev Biol 189:197–206. https://doi.org/10.1007/BF00868678

Rizki TM, Rizki RM (1980b) Properties of the larval hemocytes of *Drosophila melanogaster*. Experientia 36:1223–1226. https://doi.org/10.1007/BF01976142

Rizki TM, Rizki RM (1981) Alleles of lz as suppressors of the Bc-phene in *Drosophila melanogaster*. Genetics 97:s90

Rugendorff A, Younossi-Hartenstein A, Hartenstein V (1994) Embryonic origin and differentiation of the *Drosophila* heart. Roux's Arch Dev Biol 203:266–280. https://doi.org/10.1007/BF00360522

Saj A, Arziman Z, Stempfle D, van Belle W, Sauder U, Horn T, Dürrenberger M, Paro R, Boutros M, Merdes G (2010) A combined ex vivo and in vivo RNAi screen for notch regulators in *Drosophila* reveals an extensive Notch interaction network. Dev Cell 18:862–876. https://doi.org/10.1016/j.devcel.2010.03.013

Sanchez Bosch P, Makhijani K, Herboso L, Gold KS, Baginsky R, Woodcock KJ, Alexander B, Kukar K, Corcoran S, Jacobs T et al (2019) Adult *Drosophila* lack hematopoiesis but rely on a blood cell reservoir at the respiratory epithelia to relay infection signals to surrounding tissues. Dev Cell 51:787–803.e5. https://doi.org/10.1016/j.devcel.2019.10.017

Schaub JR, Huppert KA, Kurial SNT, Hsu BY, Cast AE, Donnelly B, Karns RA, Chen F, Rezvani M, Luu HY et al (2018) De novo formation of the biliary system by TGFβ-mediated hepatocyte transdifferentiation. Nature 557:247–251. https://doi.org/10.1038/s41586-018-0075-5

Schindelin J, Arganda-Carreras I, Frise E, Kaynig V, Longair M, Pietzsch T, Preibisch S, Rueden C, Saalfeld S, Schmid B et al (2012) Fiji: an open-source platform for biological-image analysis. Nat Methods 9:676–682. https://doi.org/10.1038/nmeth.2019

Shin M, Chang E, Lee D, Kim N, Cho B, Cha N, Koranteng F, Song JJ, Shim J (2024) Drosophila immune cells transport oxygen through PPO2 protein phase transition. Nature 631(8020):350–359. https://doi.org/10.1038/s41586-024-07583-x

Shrestha R, Gateff E (1982) Ultrastructure and cytochemistry of the cell types in the larval hematopoietic organs and hemolymph of *Drosophila melanogaster*. Dev, Growth Differ 24:65–82. https://doi.org/10.1111/j.1440-169X.1982.00065.x

Sica A, Mantovani A (2012) Macrophage plasticity and polarization: in vivo veritas. J Clin Investig 122:787–795. https://doi.org/10.1172/JCI59643

Sinenko SA, Mandal L, Martinez-Agosto JA, Banerjee U (2009) Dual role of wingless signaling in stem-like hematopoietic precursor maintenance in *Drosophila*. Dev Cell 16:756–763. https://doi.org/10.1016/j.devcel.2009.03.003

Slack JMW (2007) Metaplasia and transdifferentiation: from pure biology to the clinic. Nat Rev Mol Cell Biol 8:369–378. https://doi.org/10.1038/nrm2146

Small C, Ramroop J, Otazo M, Huang LH, Saleque S, Govind S (2014) An unexpected link between Notch signaling and ROS in restricting the differentiation of hematopoietic progenitors in *Drosophila*. Genetics 197:471–483. https://doi.org/10.1534/genetics.113.159210

Sorrentino RP, Carton Y, Govind S (2002) Cellular immune response to parasite infection in the Drosophila lymph gland is developmentally regulated. Dev Biol 243(1):65–80. https://doi.org/10.1006/dbio.2001.0542. PMID: 11846478

Spratford CM, Goins LM, Chi F, Girard JR, Macias SN, Ho VW, Banerjee U (2021) Intermediate progenitor cells provide a transition between hematopoietic progenitors and their differentiated descendants. Development 148(24):dev200216. https://doi.org/10.1242/dev.200216

Tanabe K, Ang CE, Chanda S, Olmos VH, Haag D, Levinson DF, Südhof TC, Wernig M (2018) Transdifferentiation of human adult peripheral blood T cells into neurons. Proc Natl Acad Sci USA 115:6470–6475. https://doi.org/10.1073/pnas.1720273115

Tattikota SG, Cho B, Liu Y, Hu Y, Barrera V, Steinbaugh MJ, Yoon S-H, Comjean A, Li F, Dervis F et al (2020) A single-cell survey of *Drosophila* blood. eLife 9:e54818. https://doi.org/10.7554/eLife.54818

Tepass U, Fessler LI, Aziz A, Hartenstein V (1994) Embryonic origin of hemocytes and their relationship to cell death in *Drosophila*. Development 120:1829–1837. https://doi.org/10.1242/dev.120.7.1829

Terriente-Felix A, Li J, Collins S, Mulligan A, Reekie I, Bernard F, Krejci A, Bray S (2013) Notch cooperates with Lozenge/Runx to lock haemocytes into a differentiation programme. Development 140:926–937. https://doi.org/10.1242/dev.086785

Thorel F, Népote V, Avril I, Kohno K, Desgraz R, Chera S, Herrera PL (2010) Conversion of adult pancreatic α-cells to β-cells after extreme β-cell loss. Nature 464:1149–1154. https://doi.org/10.1038/nature08894

Tiwari SK, Toshniwal AG, Mandal S, Mandal L (2020) Fatty acid β-oxidation is required for the differentiation of larval hematopoietic progenitors in *Drosophila*. eLife 9:e53247. https://doi.org/10.7554/eLife.53247

Tokusumi T, Shoue DA, Tokusumi Y, Stoller JR, Schulz RA (2009) New hemocyte-specific enhancer-reporter transgenes for the analysis of hematopoiesis in *Drosophila*. Genesis 47:771–774. https://doi.org/10.1002/dvg.20561

Vilmos P (2004) A rapid rosetting method for separation of hemocyte sub-populations of *Drosophila melanogaster*. Dev Comp Immunol 28:555–563. https://doi.org/10.1016/j.dci.2003.10.001

Vlisidou I, Wood W (2015) Drosophila blood cells and their role in immune responses. FEBS J 282:1368–1382. https://doi.org/10.1111/febs.13235

Wei C, Yu P, Cheng L (2020) Hematopoietic reprogramming entangles with hematopoiesis. Trends Cell Biol 30(10):752–763. https://doi.org/10.1016/j.tcb.2020.07.006

Wood W, Jacinto A (2007) *Drosophila melanogaster* embryonic haemocytes: masters of multitasking. Nat Rev Mol Cell Biol 8(7):542–551

Xie H, Ye M, Feng R, Graf T (2004) Stepwise reprogramming of B cells into macrophages. Cell 117:663–676. https://doi.org/10.1016/s0092-8674(04)00419-2

Zhou L, Chong MMW, Littman DR (2009) Plasticity of CD4+ T cell lineage differentiation. Immunity 30:646–655. https://doi.org/10.1016/j.immuni.2009.05.001

Zhou X, von der Mark K, Henry S, Norton W, Adams H, de Crombrugghe B (2014) Chondrocytes transdifferentiate into osteoblasts in endochondral bone during development, postnatal growth and fracture healing in mice. PLoS Genet 10(12):e1004820. https://doi.org/10.1371/journal.pgen.1004820

Acknowledgements

Author contributions

Disclosure and competing interests statement

Expanded View Figures

Figure EV1. Notch activity in cortical plasmatocytes and co-localization of P1 with crystal cell markers.

(A) Hml-CytoplasmicDsRed was used to mark mature haemocytes of the cortical region and NRE-eGFP as a reporter of Notch activation. NRE-eGFP expression is restricted to the cortical region of the lymph gland showing that Notch activation is restricted to mature and maturing plasmatocytes. Beneath the main image is a XZ slice of the same lymph gland illustrating the specificity of the two markers to the cortical region. Dotted lines define the contour of the primary lymph gland lobes. (a') Shows an orthogonal section of the Lymph glands shown in (A). The horizontal dashed line in (A) represents the location of the slice. (B) Bc-GFP lymph glands stained with anti-Nimrod (red). Bc-GFP is a marker of crystal cells that co-localizes in a subset of cortical cells with the plasmatocyte marker Nimrod (P1) (white arrowheads). Dotted lines define the contour of the primary lymph gland lobes. (b') 10-fold magnification of the inset in (B). (C) Lz-Gal4, UAS-GFP lymph glands stained with P1 (anti-Nimrod) (red). In agreement with the staining in (A), double-positive cells can be observed in the cortical region of the lymph gland (white arrowheads). Dotted lines define the contour of the primary lymph gland lobes. (c') 10-fold magnification of the inset in (C). Scale bars represent 100 μm in (A–C), and 10 μm in (a'–c').
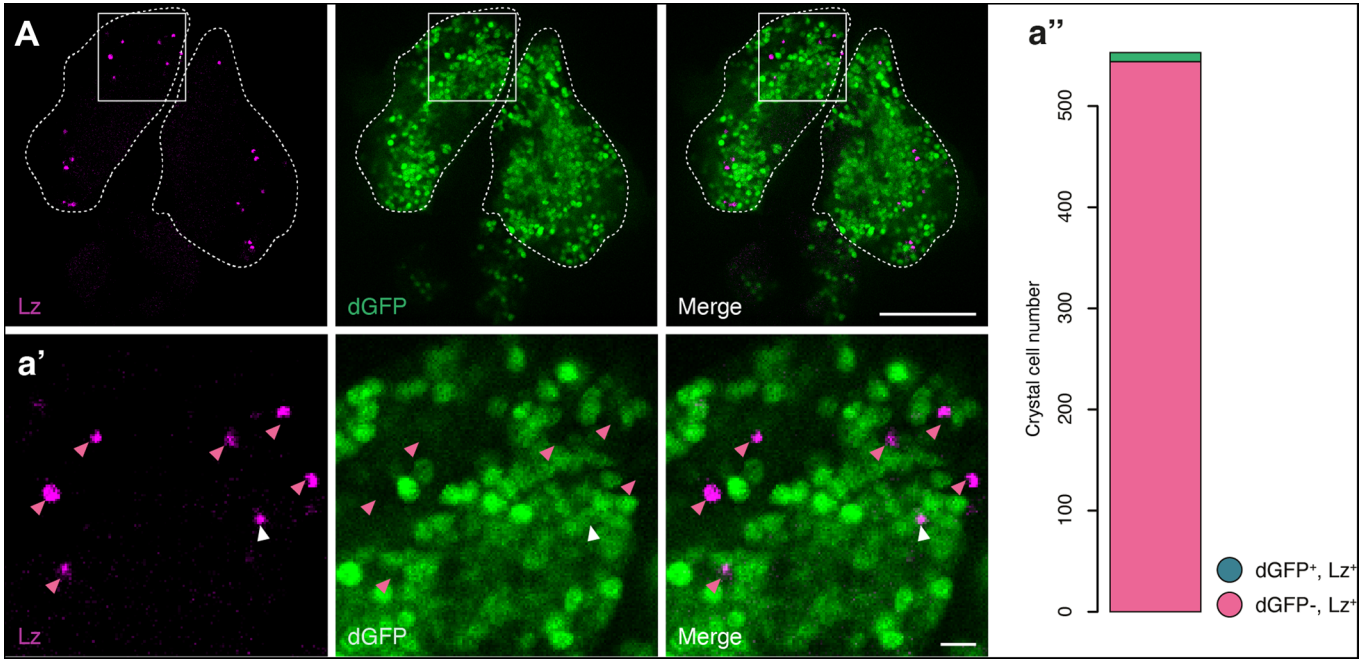
▶
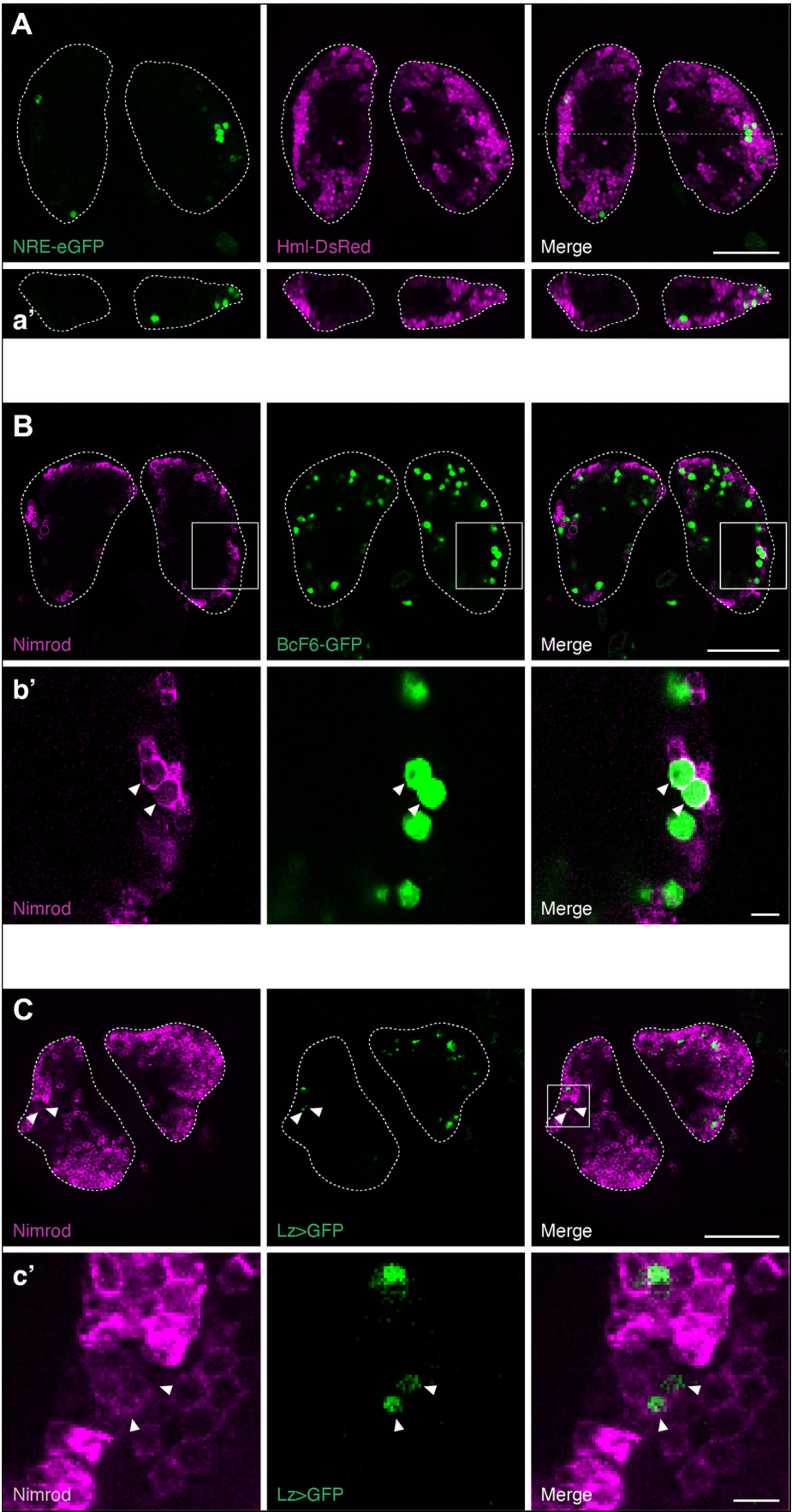
Figure EV2. Eater-Gal4 expression is rapidly lost in Crystal cells.

Eater-Gal4 driving destabilized GFP expression is lost rapidly in crystal cells as shown by the lack of co-localization with Lozenge. Dotted lines define the contour of the primary lymph gland lobes. (a') 10-fold magnification of the inset in (**A**). Magenta arrows mark cells positive for Lz alone. Rare double-positive cells are marked by white arrows. (a'') Scale bar represents 100 μm in (**A**) and 10 μm in (a').
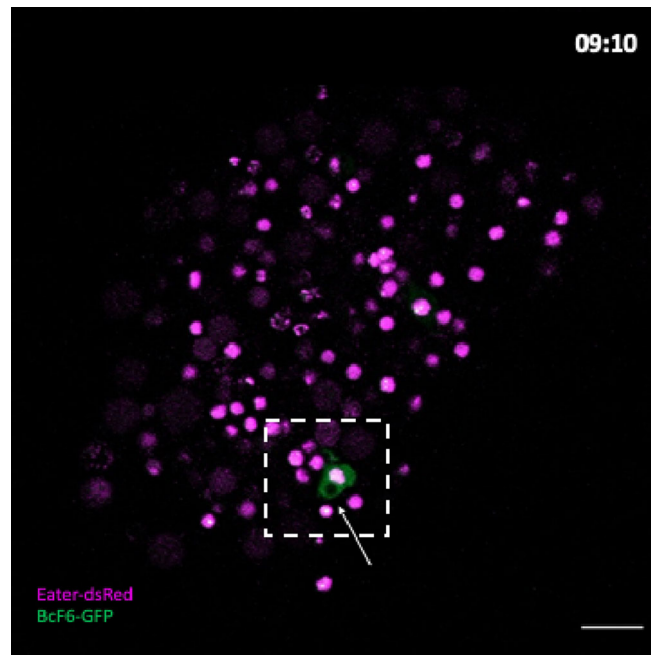
Figure EV3. "Dark spots" observed in double-positive cells from cultured lymph glands.

Image extracted from timelapse represented in Movie EV1. At around 9 h of culture, "dark spots" were observed within the BcF6-GFP expression domain of a double-positive cell (inside white dotted box), suggesting PPO1 production by transdifferentiating cells. Scale bar represents 20 μm.
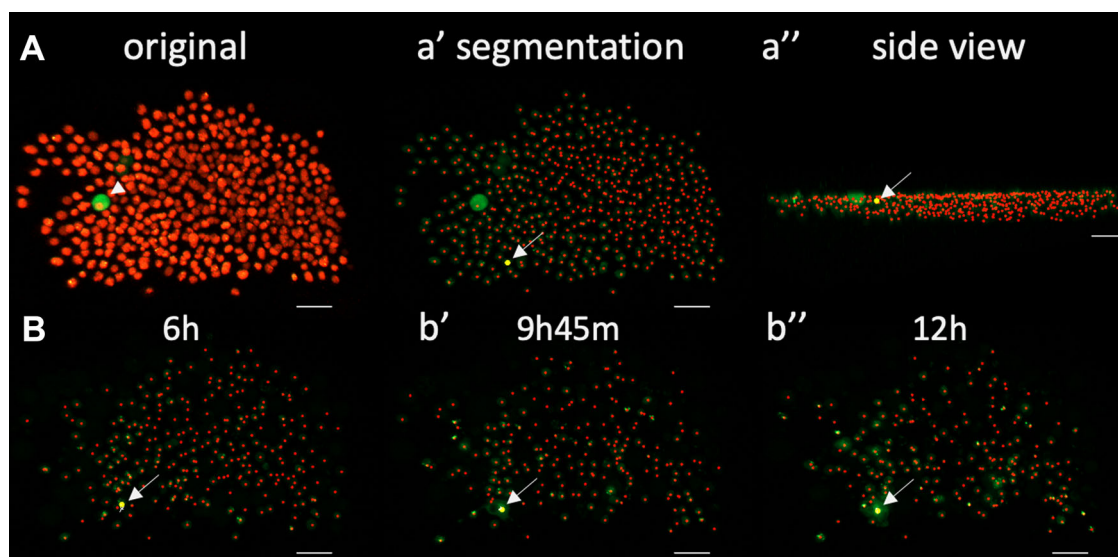
Figure EV4. Transdifferentiation of plasmatocytes into crystal cells can occur in the cortical zone of the lymph gland.

(A) Lymph gland from Movie EV1 with *Eater*-DsRed and BcF6-GFP markers. Crystal cells can be observed with cytoplasmatic GFP signal (green arrowhead). (a') Spot segmentation of DsRed nuclei allows the tracking of individual cells throughout the experiment. Two *Eater*-DsRed[+] BcF6-GFP^{-} cells are highlighted with a white spot and arrow. Both these nuclei are in the second row of nuclei from the surface of the lymph gland. (a") At 12 h the cytoplasm around these nuclei is GFP[+]. (B) An independent sample of lymph gland ex vivo culture, with examples of BcF6-GFP[+] marked with green arrows. (b') At 0 h, it is possible to identify 4 *Eater*-DsRed[+] BcF6-GFP^{-} cells that will gain GFP expression. Two of these cells are in the second row of nuclei (arrows) and the other two are deeper in the tissue (white arrowheads). (b") At 12 h the cytoplasm around these nuclei is GFP[+]. Scale bars represent 15 μm (A, a', a") and 10 μm (B, B', B").
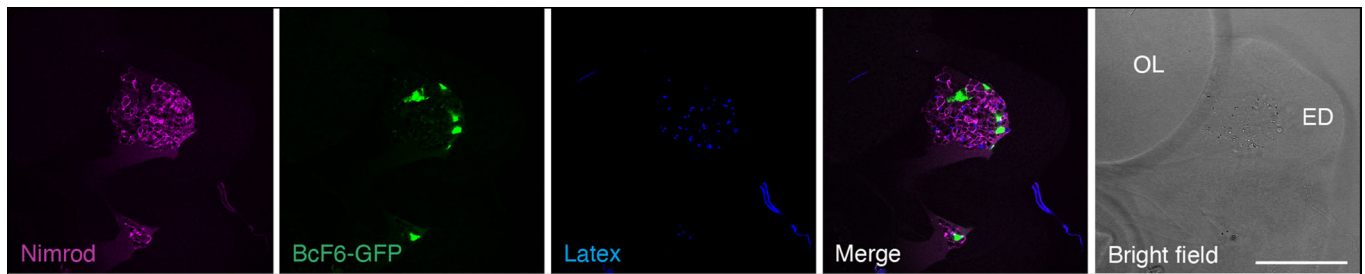
Figure EV5. Latex beads are taken up exclusively by haemocytes.

Latex beads co-localize only with the haemocyte patch (outlined in white) identified by the expression of Bc (crystal cells) or P1 (plasmatocytes). Cells of the neighboring eye disc (ED) and optic lobe (OL), visible in the merge image, show no phagocytosis of the latex beads. Scale bar represents 100 μm.
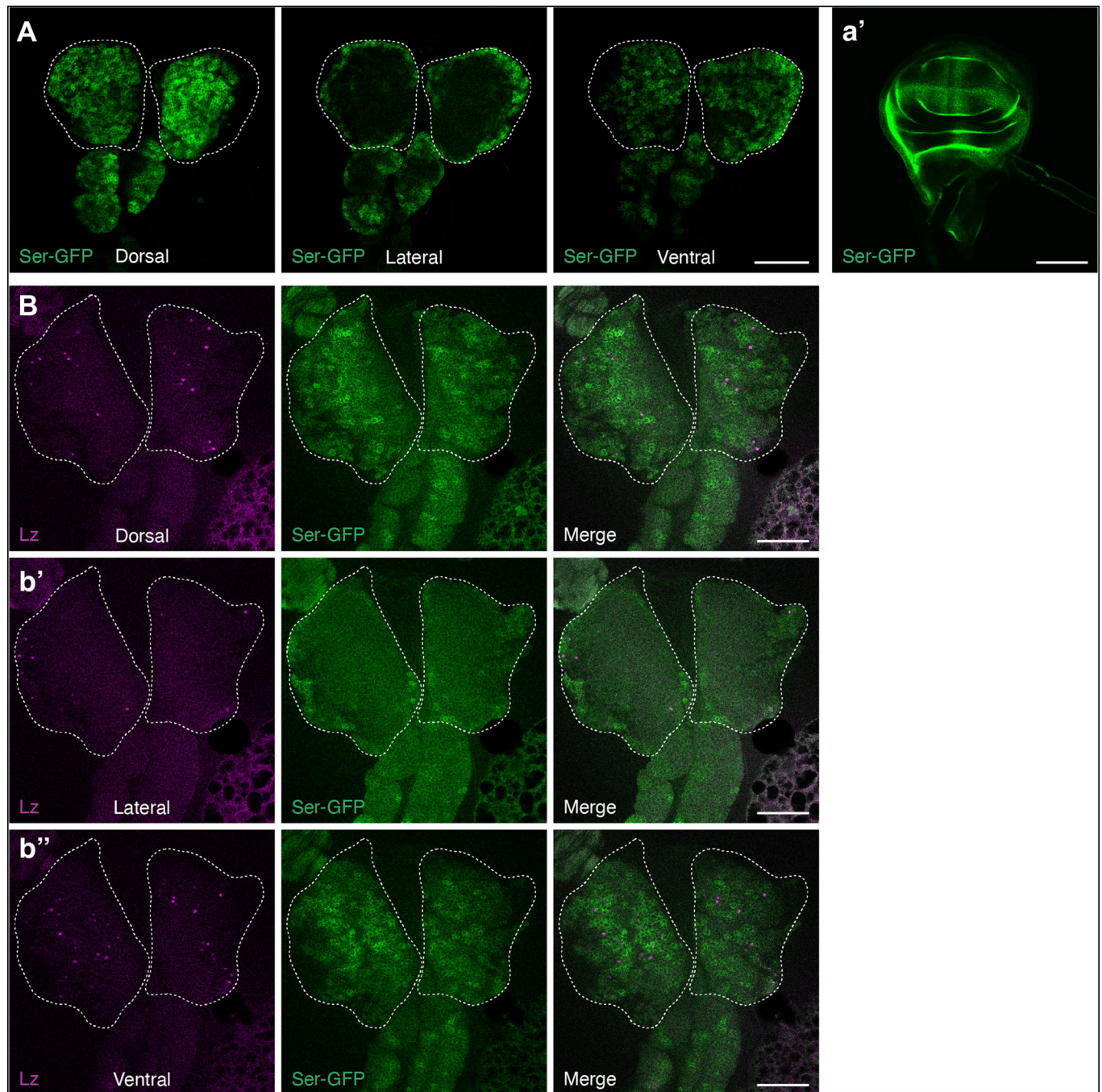
Figure EV6. Serrate expression in the larval lymph gland.

A Serrate eGFP protein fusion (Nagarkar-Jaiswal et al, 2015) appears restricted to a shallow layer of cortical plasmatocytes (**A**, **B**, **b'**, **b''**) and absent in the medullary prohaemocytes (**a'**, **b'**) of L3 larvae imaginal discs. This Ser-GFP fully recapitulates the endogenous expression in the wing disc when compared to published Serrate immunostainings (Lai, 2005) based on its pattern in the wing imaginal disc (**a'**). Crystal cell differentiation (revealed with anti-Lz) is limited to regions of Serrate expression (**B**, **b'**, **b''**). Dotted lines define the contour of the primary lymph gland lobes. Scale bars represent 100 μm.